Petrology, Vol. 13, No. 4, 2005, pp. 322–351. Translated from Petrologiya, Vol. 13, No. 4, 2005, pp. 358–388.

Petrology of Avachites, High-Magnesian Basalts of Avachinsky Volcano, Kamchatka: II. Melt Inclusions in Olivine

M. V. Portnyagin*,,***, N. L. Mironov**, S. V. Matveev****, and P. Yu. Plechov*******

**IfM-GEOMAR, Division of the Ocean Floor, Wischhofstr. 1–3, Kiel, Germany*
e-mail: mportnyagin@ifm-geomar.de
***Vernadsky Institute of Geochemistry and Analytical Chemistry (GEOKhI), Russian Academy of Sciences, ul. Kosygina 19, Moscow, 119991 Russia*
e-mail: nmironov@geokhi.ru
****Institute of Volcanology and Seismology, Far East Division, Russian Academy of Sciences, bul'v. Piipa 9, Petropavlosk-Kamchatskii, 683006 Russia*
*****University of Alberta, 1-26 Earth Sciences Building, Edmonton, Canada*
******Faculty of Geology, Moscow State University, Vorob'evy gory, Moscow, 119899 Russia*

Received July 15, 2004

Abstract—The composition and crystallization conditions of the parental melts of avachites were elucidated by studying melt inclusions in olivine ($Fo_{85.8–90.7}$) phenocrysts. The melt inclusions captured during the crystallization of primitive magmas subsequently reequilibrated with their host minerals and became partly recrystallized and decrepitated. The diffusion-controlled reequilibration of the melt inclusions with the olivine occurred at temperatures close to ~1100°C and was associated with the crystallization of daughter phases: olivine, high-Ca pyroxene, and spinel. The composition of the pyroxene and spinel in the inclusions evolved toward extremely high Al contents, which is atypical of pyroxene in the rocks and was controlled by plagioclase absence from the daughter phase assemblage of the inclusions. Magma decompression induced the partial decrepitation of the melt inclusions, a process that was associated with the escape of fluid components (CO_2 and H_2O) and variable amounts of the residual silicate material from the inclusions. The initial compositions of the melt inclusions, which were reconstructed using techniques of experimental homogenization and modeling, show broad ranges in the contents of major and trace elements. Compared with the composition of the rocks, the compositions of inclusions in the olivine $Fo > 90\%$ are higher in CaO, Al_2O_3, and Na_2O at lower concentrations of SiO_2. Their geochemical characteristics are identical to those of low-Si ankaramite melts occurring in many island arcs. The carbonatite metasomatism of the arc mantle, the derivation of nepheline-normative ankaramite magmas, and the significant crustal contamination of these magmas during their fractionation can be spread more widely than is currently assumed in models for island-arc petrogenesis. The evolution of the avachite primitive magmas was controlled by the crystallization of early olivine, high-Ca pyroxene, spinel, and, perhaps, the assimilation of crustal rocks in the magmatic chambers at different depths (from 5 to 30 km). During two (or more) crystallization stages, olivine–pyroxene cumulates were produced, remobilized, and transported to the surface by the differentiated hypersthene-normative magmas. Avachites are hybrid cumulative rocks, which were produced in a long-lived open magmatic system.

1. INTRODUCTION

Elucidation of the composition of parental arc magmas and the conditions under which they were derived and evolved is a fundamental petrological and geochemical problem. When solved, this problem (i) offers the possibilities to evaluate the composition of the continental crust generated in active continental margins (Gill, 1981), (ii) provides insight into an important stage in the Earth's mantle evolution and the recycling of the crustal material (Hofmann, 1997), and (iii) furnishes an independent criterion for assaying the evolutionary dynamics of the thermal state of the mantle above subduction zones (Tatsumi *et al.*, 1983). The composition of primitive arc magmas can be estimated by studying the chemistries of primitive rocks, their minerals, and magmatic inclusions in these minerals. The traditional approach with the use of the compositions of rocks is currently predominant in geology because of the simplicity and intuitively clear interpretation of the rocks as samples of deep magmas and the availability of the wealth of analytical techniques (for the comprehensive characterization of the chemical

compositions) and well-developed methods of thermo- and barometry. The principal disadvantage of this approach stems from the fact that igneous rocks are always the final products of a complex magma evolution (see, for example, O'Hara and Herzberg, 2002), which, however, sometimes cannot be reproduced unambiguously. Because of this, the attention of researchers has long been attracted to melt inclusions in minerals, more specifically, to the unique ability of these inclusions to be isolated by the host mineral from all evolutionary processes in the magmatic system (such as crystallization, assimilation, mixing, and degassing) that determine the final characteristics of the rocks and modify the composition of their parental magmas. Studying melt inclusions potentially enables the researcher to reconstruct the initial and intermediate evolutionary stages of the magmatic system. The progress in the development of precise analytical techniques with a high spatial resolution over the past decade triggered the revival of keen interest in studying melt inclusions (Sobolev, 1996; Frezotti, 2001; Danyushevsky *et al.*, 2002a). However, the reliability of such data is still (as a century ago) sometimes questioned, because the parameters of vast magmatic systems are inferred from information on micrometer-sized inclusions, whose capture mechanisms and further compositional evolution are still not fully understood (Qin *et al.*, 1992; Tait, 1992; Gaetachi and Watson, 2000; Danyushevsky *et al.*, 2000, 2002a).

This paper presents the results of a detailed study of melt inclusions in olivine from avachites, a rare variety of high-Mg basalts from Kamchatka (see, for example, Kutyev *et al.*, 1980). We demonstrate that several processes responsible for the origin and evolution of the composition of these inclusions can be deciphered using currently available microanalytical techniques and mathematical simulations. The compositions of melt inclusions provide principally new information on the genesis of avachites. The results of our research and independent data of other investigations call for revising the preexisting interpretations of primitive arc basalts as samples of undifferentiated mantle magmas. The derivation of nepheline-normative ankaramite magmas and their significant crustal assimilation during fractionation could be processes spread more widely than is assumed in modern models for arc magmatism.

2. SAMPLES STUDIED

Avachites are olivine–clinopyroxene coarsely porphyritic basalts and picrites (SiO_2 = 49.4–52.6 wt %, MgO = 14–20 wt %), which were found in the isthmus between Avachinsky and Kozel'sky volcanoes at the southern termination of the Eastern Segment of the Kamchatkan Volcanic Belt (Kutyev *et al.*, 1980). The petrography, mineralogy, and geochemistry of these rocks, which are unique for Kamchatka and very rare in island arcs elsewhere, are described in detail in (Portnyagin *et al.*, 2005). Along with their unusual bulk composition (Table 1), avachites are noted for the extremely primitive composition of their liquidus mineral assemblage, which consists of olivine (Fo_{91}), clinopyroxene (Mg# = 92.5 mol %), and Cr-spinel [Cr/(Cr + Al) = 0.82]. These minerals supposedly started to crystallize simultaneously under a pressure of

Table 1. Average composition (wt %) of avachites, their parental melts, and groundmasses; the composition parameters and equilibrium conditions of liquidus minerals

Component	1	2	3	4	5
	Avach	GM	AV-91	AV-94	AV-I
SiO_2	51.4	54.9	52.1	50.5	47.4
TiO_2	0.52	0.75	0.62	0.5	0.72
Al_2O_3	9.8	16.1	11.9	10.1	14.4
FeO*	8.2	8.4	8.4	8.2	8.0
MnO	0.16	0.10	0.16	0.1	0.11
MgO	16.3	5.8	13.1	18.9	10.4
CaO	11.7	10.4	11.1	9.4	15.5
Na_2O	1.6	2.9	2.0	1.63	2.7
K_2O	0.36	0.60	0.46	0.43	0.63
P_2O_5	0.11	0.15	0.14	0.12	0.18
Fo, mol %		80	91	94	90.5
Mg# *Cpx*, mol %		78	92.5		~92
T, °C		~1050	~1300	~1400	~1270
P, GPa		~0.1	~1	~2	~0.6
CIPW norm					
Qtz	–	3.5	–	–	–
Pl	31.9	53.4	38.9	32.8	29.1
Or	2.1	3.6	2.7	2.5	3.7
Ne	–	–	–	–	10.3
Di	31.1	17.6	25.6	21.6	40.8
Hy	17.2	20.2	21.5	17.8	–
Ol	16.5	0.0	9.8	23.9	14.3
Ilm	1.0	1.4	1.2	1.0	1.4
Ap	0.3	0.4	0.3	0.3	0.4

Note: (1) Average composition of avachites; (2) calculated composition of the groundmass of avachites; (3) and (4) parental melts in equilibrium with olivine Fo_{91} and Fo_{94}, respectively, calculated from the compositions of the rocks; (5) parental melts of avachites based on data on melt inclusions in olivine *Fo* > 90 mol %. All compositions are recalculated to anhydrous residue. FeO* is the total Fe in the form of FeO. *Fo* is the composition (mol %) of liquidus olivine; Mg# = 100Mg/(Mg + Fe), Mg mole fraction of liquidus pyroxene; *T* and *P* are the equilibrium temperature and pressure. The compositions and conditions (*T*, *P*) of equilibria between melts with olivine and pyroxene are given according to data from (Portnyagin *et al.*, 2005) (compositions 1–4) and this paper (composition 5).

1.0 GPa and a temperature of about 1300°C. The parental melts of avachites could be hydrous high-Mg basaltic (MgO ~ 13 wt %) or even picritic liquids, whose geochemical characteristics were intermediate between those of arc ankaramites and high-Ca boninites. The parental melts of avachites could be generated by the partial melting of depleted lherzolite under pressures of more than 1.0 GPa, with the participation of a component (fluid or melt) rich in incompatible elements, a process that predetermined the anomalous enrichment of avachites in both strongly incompatible (Ba, Th, Sr, and LREE) and refractory (Cr, Ni, and Os) elements.

Many geochemical features of avachites can be explained within the framework of a simple geochemical model for the crystallization of the parental magmas in a closed system (Portnyagin *et al.*, 2005). The key points of this model are as follows: (i) the mafic minerals occur in nature in cotectic proportions and are merely insignificantly accumulated relative to their calculated contents during melt crystallization in a closed system; and (ii) the rock groundmass is the final product of the polybaric crystallization of olivine, pyroxene, and spinel from the parental melt. Nevertheless, some observations cannot be explained within the scope of such a model. These facts are the occurrence of unzoned olivine phenocrysts with broad compositional variations in the rock, the complicated zoning of the pyroxene, and the unusual IR absorption spectra of the OH^- group in the olivine structure, which suggest that the parental magmas were strongly undersaturated in silica, in contrast to the compositions of the rocks themselves and to the compositions of the parental melts calculated based on the compositions of the rocks. These facts led us (Portnyagin *et al.*, 2005) to hypothesize that avachites could have been of hybrid cumulative genesis. This paper reports the results of testing of this hypothesis using the data obtained by studying melt inclusions in olivine from avachites.

3. METHODS

3.1. Experimental Techniques

In order to determine the bulk composition of recrystallized melt inclusions, we applied the method of partial experimental homogenization (Danyushevsky *et al.*, 2002a). The experiments were conducted at the Vernadsky Institute on a heating stage designed for microthermometric research by A.V. Sobolev and A.B. Slutsky (Sobolev *et al.*, 1980). All of experiments were carried out under atmospheric pressure in a medium of highly pure helium, which was additionally purified from oxygen-bearing admixtures on a $Zr–ZrO_2$ getter at a temperature of 800°C. A light inert gas was used in the experiments to preclude olivine oxidation at the high temperature and because of the rapid convection of this gas that ensured the effective quenching of the material after termination of the experiment. The temperature at the heater was measured with a $Pt–PtRh_{10}$ thermocouple, which was calibrated in each experiment against the gold melting point (1064°C). During the experiments, doubly polished platelets of individual olivine grains were heated to the melting temperature of the daughter pyroxene crystal or to a slightly higher temperature (1200–1280°C), held at this temperature for 10–15 min to homogenize the melt in the inclusion, and quenched by switching off the heater and the simultaneous switching on the helium flow through the heating stage. The heating rate was approximately 10–20°C/min because of the slow melting of the material of the inclusions. The complete homogenization was not achieved in any of the experiments, so that inclusions after quenching contained gas bubbles (5–10% by volume) and, often, small (<1 vol %) spinel crystals. After the experiments, the platelets were polished until the inclusions became exposed at the surfaces, and the latter were analyzed for major, trace, and volatile components.

3.2. Analytical Techniques

The composition of inclusions and their host minerals before and after the experiments were analyzed in epoxy pellets that were polished by diamond and corundum pastes. The compositions of minerals and glasses were determined on a Camebax-microbeam, Cameca SX-50, and JEOL JXA 8900RL microprobes (at the Vernadsky Institute in Moscow, IfM-GEOMAR in Kiel, and the Geochemical Institute in Göttingen, respectively). The analyses were conducted at an accelerating voltage of 15 kV and a current of 10–15 nA for glasses and 30 nA for minerals. Minerals were analyzed at the maximum focusing of the beam, and glasses were analyzed in scanning mode (in Moscow and Kiel) or by a defocused beam (in Göttingen) over an area of 5–10 μm. Each analysis published in this paper is an average of 3–5 individual analyses. The errors were typically less than 1 rel. % for major elements and 5–10 rel. % for concentrations of less than 1 wt %. The calibration was performed by analyzing natural standards of olivine (USNM 11312/444), augite (USNM 12214), chromite (USNM 117075), and glass (USNM 111240/52 VG-2) (Jarosewich *et al.*, 1980). The peak and background counting times were 20/10 s for major elements and 60/30 s for P, S, and Cl. Analyses for Cl were calibrated on NaCl. The secondary standards for monitoring the accuracy of the analyses were KE-3 and KN-18 glasses (Mosbah *et al.*, 1991) and scapolite (USNM R6600-1) (Jarosewich *et al.*, 1980). The S concentrations were determining with regard for the dependence of the wavelength of the X-ray radiation of this element on its valence (Wallace and Carmichael, 1992; Metrich and Clocchiatti, 1996). It was determined that all S contained in the glasses was (within the analytical accuracy) in the reduced state (S^{2-}). The measurements were calibrated on synthetic standards of sphalerite (S^{2-}) and barite (S^{6+}). The secondary standards were basaltic glasses VG-2 [S = 1420 ppm, Wallace and Car-

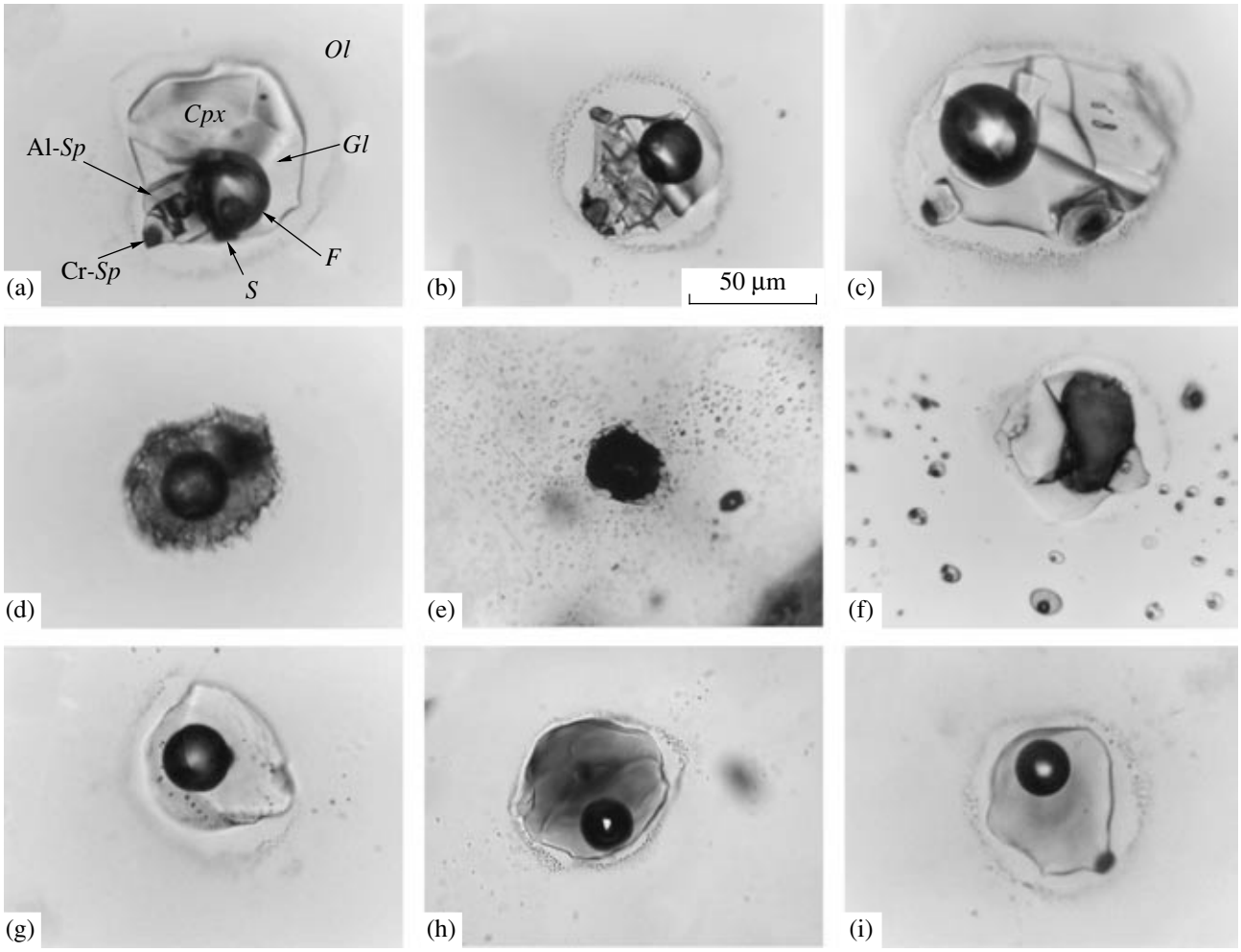

Fig. 1. Micrographs of melt inclusions in olivine from avachites.
(a)–(c) Coarsely crystalline melt inclusions in olivine. Phases: *Ol*—olivine, *Cpx*—daughter clinopyroxene, *Gl*—glass, Al-*Sp*—aluminous spinel, Cr-*Sp*—chromian spinel, *S*—sulfide, *F*—fluid.
(d) Finely crystalline inclusion (*Gl* + *F* + *Cpx*).
(e) Decrepitated fluid inclusion.
(f) Decrepitated melt inclusion.
(g)–(i) Partly homogenized melt inclusions.

michael, 1992; S = 1454 ± 50 ppm (1σ), this study], ALV983R23 [S = 1110 ppm, Metrich and Clocchiatti, 1996; S = 1122 ± 60 ppm, this study], and scapolite R6600-1 [S = 5280 ppm, Jarosewich *et al.*, 1980; S = 5850 ± 250 ppm, this study].

The contents of trace elements in melt inclusions were determined by SIMS on a Cameca ims-4f at the Institute of Microelectronics, Russian Academy of Sciences, in Yaroslavl. The method is described in detail in (Sobolev, 1996). The analytical accuracy of this technique is 10–15 rel. % at concentrations higher than 1 ppm and 15–30 rel. % at concentrations of 0.1–1 ppm. The detection limits for different elements are 0.01–0.001 ppm.

4. MORPHOLOGY OF INCLUSIONS AND THEIR PHASE COMPOSITION

Magmatic inclusions in the olivine are melt, fluid, and crystalline (spinel and pyroxene, Fig. 1). The inclusions comprise two generations. Primary inclusions are rare; they are large and chaotically distributed in the host olivine grains. Abundant secondary fluid and melt inclusions occur as flat swarms in the planes of healed cracks in olivine grains. The composition of crystalline inclusions was described in much detail in (Portnyagin *et al.*, 2005). All of the fluid inclusions examined in the samples appeared to have been unsealed (Fig. 1e). The very low fluid density did not allow us to draw any conclusions about the contents of the inclusions from the results of cryometric experiments. In this paper, much

Table 2. Representative analyses (wt %) of the daughter phases of melt inclusions and compositions (wt %) of phases in the rock groundmass

Component	Inclusion 6					Inclusion 7					Inclusion 2				Groundmass	
	Cpx core	*Cpx* rim	*Gl*	*Spl*	*Ol*	*Cpx* core	*Cpx* rim	*Gl*	*Spl*	*Ol*	*Cpx* core	*Cpx* rim	*Gl*	*Ol*	*Cpx*	*Gl*
SiO_2	49.95	45.75	64.09	0.56	40.78	50.35	45.44	64.07	0.66	40.53	52.26	47.15	64.4	40.16	51.30	76.73
TiO_2	0.57	1.2	0.66	0.2		0.49	1.19	0.54	0.27		0.34	1.01	0.6		0.63	1.50
Al_2O_3	6.55	10.95	23.63	60.61		6.04	10.52	22.54	53.89		2.76	10.14	22.36		2.08	10.19
FeO*	5.41	6.76	0.65	12.45	9.35	5.76	7.01	0.49	13.55	9.32	3.1	6.19	0.87	10.96	11.08	1.70
MnO	0.1	0.04	0.00	0.07	0.24	0.04	0.13	0.06	0.07	0.16	0.12	0.06	0.05	0.13	0.22	0.03
MgO	13.94	11.71	0.52	20.83	49.65	14.56	11.88	0.55	19.47	49.55	16.95	12.95	0.71	48.73	15.56	0.08
CaO	23.22	23.67	0.76		0.17	22.63	23.56	0.36		0.21	23.17	23.14	1.53	0.19	18.24	1.35
Na_2O	0.29	0.33	8.15			0.27	0.42	7.98			0.27	0.37	7.75		0.45	3.14
K_2O			2.69					2.63					1.88			3.39
P_2O_5			0.36					0.41					0.39			
Cl			0.57					0.49					0.42			
NiO										0.27						
Cr_2O_3	0.54	0.04		1.39	0.26	0.75	0.16		9.72		0.98	0.23		0.18		
Total	100.57	100.45	102.08	96.11	100.45	100.89	100.31	100.12	97.63	100.04	99.95	101.24	100.96	100.35	99.56	98.11
Mg#, mol %	82.1	75.5	58.8	74.9	90.4	81.8	75.1	66.7	71.9	90.5	90.7	78.9	59.3	88.8	71.5	7.3
T, °C		1109					1150					1116				
P, GPa		0.35					0.57					0.35				
Pyroxene end members, mol %																
Jd + *Ac*	2.1	2.4				1.9	3.0				1.9	2.6		3.3		
FeCa-*Ts*	3.7	11.5				4.1	15.5				4.8	10.3		5.2		
CrCa-*Ts*	1.6	0.1				2.2	0.5				2.8	0.7		0		
CaTi-*Ts*	1.6	3.3				1.3	3.3				0.9	2.8		1.8		
Ca-*Ts*	8.9	13.4				7.5	10.0				0.2	12.1		0		
Di + *Hd*	75.3	64.9				73.2	63.6				81.6	64.2		65.9		
En + *Fs*	7.0	4.4				9.7	4.0				7.7	7.3		23.9		

Note: Here and in Table 3 FeO* is total iron as FeO. Average compositions of pyroxene and glass in the groundmass of avachites are according to (Portnyagin *et al.*, 2005). The temperature and pressure of equilibrium between pyroxene and melt were calculated by the model from (Putirka *et al.*, 1996). Pyroxene end members: *Jd*—$NaAlSi_2O_6$, *Ac*—$NaFe^{3+}Si_2O_6$, FeCa-*Ts*—$CaFe^{3+}AlSiO_6$, CrCa-*Ts*—$CaCrAlO_6$, CaTi-*Ts*—$CaTiAl_2O_6$, Ca-*Ts*—$CaAl_2SiO_6$, *Di*—$CaMgSi_2O_6$, *Hd*—$CaFeSi_2O_6$, *En*—$Mg_2Si_2O_6$, *Fs*—$Fe_2Si_2O_6$. Analyses were conducted at Vernadsky Institute of Geochemistry and Analytical Chemistry, Russian Academy of Sciences. * Phases: *Cpx*—clinopyroxene, *Gl*—glass, *Spl*—spinel, *Ol*—host olivine.

attention is focused on the composition of the primary melt inclusions.

Primary melt inclusions in the olivine are rare. Large inclusions from 30 to 150 μm across are round, ellipsoidal, or, sometimes, flattened and always partly recrystallized. Inclusions in the high-Mg olivine ($Fo_{87–91}$) consist of single euhedral crystals of daughter phases: high-Ca pyroxene, spinel, a fluid bubble, and, sometimes, a sulfide phase, submerged in glass of trachydacite composition (Table 2, Figs. 1a–1c). Some inclusions in the relatively ferrous olivine ($Fo_{85–87}$) have a microlitic texture and consist of randomly oriented acicular pyroxene grains and glass (Fig. 1d).

The residual glasses of the inclusions have trachytic composition (SiO_2 = 60–68 wt %, Na_2O = 6.6–9.0 wt %, K_2O = 1.4–2.7 wt %) and a stoichiometry approaching those of alkali feldspars. Compared with the compositions of inclusions in the rock groundmasses and melt inclusions in plagioclase in lavas of Avachinsky volcano (Tolstykh *et al.*, 2002), the glasses of the melt inclusions are poorer in SiO_2, FeO*[1], TiO_2, and K_2O and much richer in Al_2O_3, Na_2O, and Cl (Table 2, Fig. 2). Although the MgO and FeO contents in the glasses do not exceed 1 wt %, their Mg# [Mg# = Mg/(Mg + Fe)] is unusually high (59–67 mol %) for such differentiated compositions.

Clinopyroxene in the inclusions is magnesian (Mg# = 75–91 mol %), corresponding to the compositional range of the phenocrysts, and strongly zoned (Table 2, Fig. 3). The cores of the crystals are often highly magnesian and low aluminous, analogously to the composition of phenocrysts and crystalline inclusions of pyroxene in olivine. The composition of the marginal, most ferrous zones of the daughter pyroxenes is very unusual and is characterized by extremely low contents of SiO_2 (42–46 wt %) and high contents of CaO (22–23.5 wt %), TiO_2 (1–2 wt %), and Al_2O_3 (8–16 wt %). These compositional characteristics of the daughter pyroxenes make them principally different from pyroxene phenocrysts in avachites and the groundmass pyroxene in these rocks. The Na_2O concentrations (0.3–0.5 wt %) in the marginal zones of the pyroxenes are slightly higher than in their cores but remain within the compositional range of the phenocrysts. The conditions of equilibrium between the pyroxene margins and residual glass in the inclusions were evaluated at 1109–1150°C and 0.35–0.57 GPa (Putirka *et al.*, 1996). Because of their unusual composition, pyroxenes in the melt inclusions were sometimes mistaken for garnet (see, for example, Anan'ev and Shnyrev, 1984). However, the optical properties and calculated stoichiometry of this mineral unambiguously indicate that it is clinopyroxene extremely rich in the tschermakite component (30–40 mol %; Fig. 4, Table 2), while the pyroxene phenocrysts contain no more than 15 mol % of the sum of tschermakite components.

[1] Hereafter FeO* is total iron as FeO.

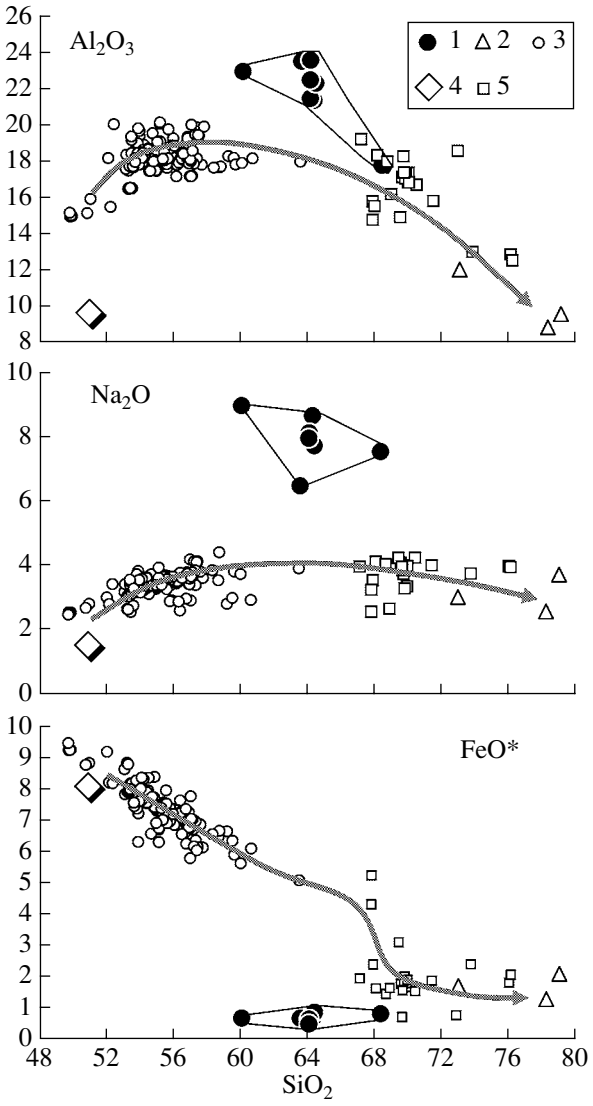

Fig. 2. Composition of residual glasses in melt inclusions. (1) Glasses in partly recrystallized melt inclusions; (2) volcanic glass in the groundmass of avachites; (3) lavas of Avachinsky volcano (Castellana, 1998); (4) average composition of avachites; (5) melt inclusions in plagioclase from lavas of Avachinsky volcano (Tolstykh *et al.*, 2002). Oxide concentrations are recalculated to anhydrous residue and expressed in wt %. The heavy line with an arrow corresponds to the fractionation path of the Avachinsky magmas, as inferred from the composition of the rocks, melt inclusions in plagioclase, and groundmass glass of avachites.

Spinel crystals in the inclusions commonly have brown cores (chromite), whose composition is close to that of crystalline spinel inclusions in olivine. The peripheral portions of the crystals consist of pale green high-Al [Cr/(Cr + Al) = 0.02–0.11), low-Ti (TiO_2 = 0.2–0.3 wt %) spinel (Table 2, Figs. 1a–1c), which was not found among crystalline inclusions in the olivine (Portnyagin *et al.*, 2005).

Summarizing the compositional features of the inclusions, it should be mentioned that the daughter cli-

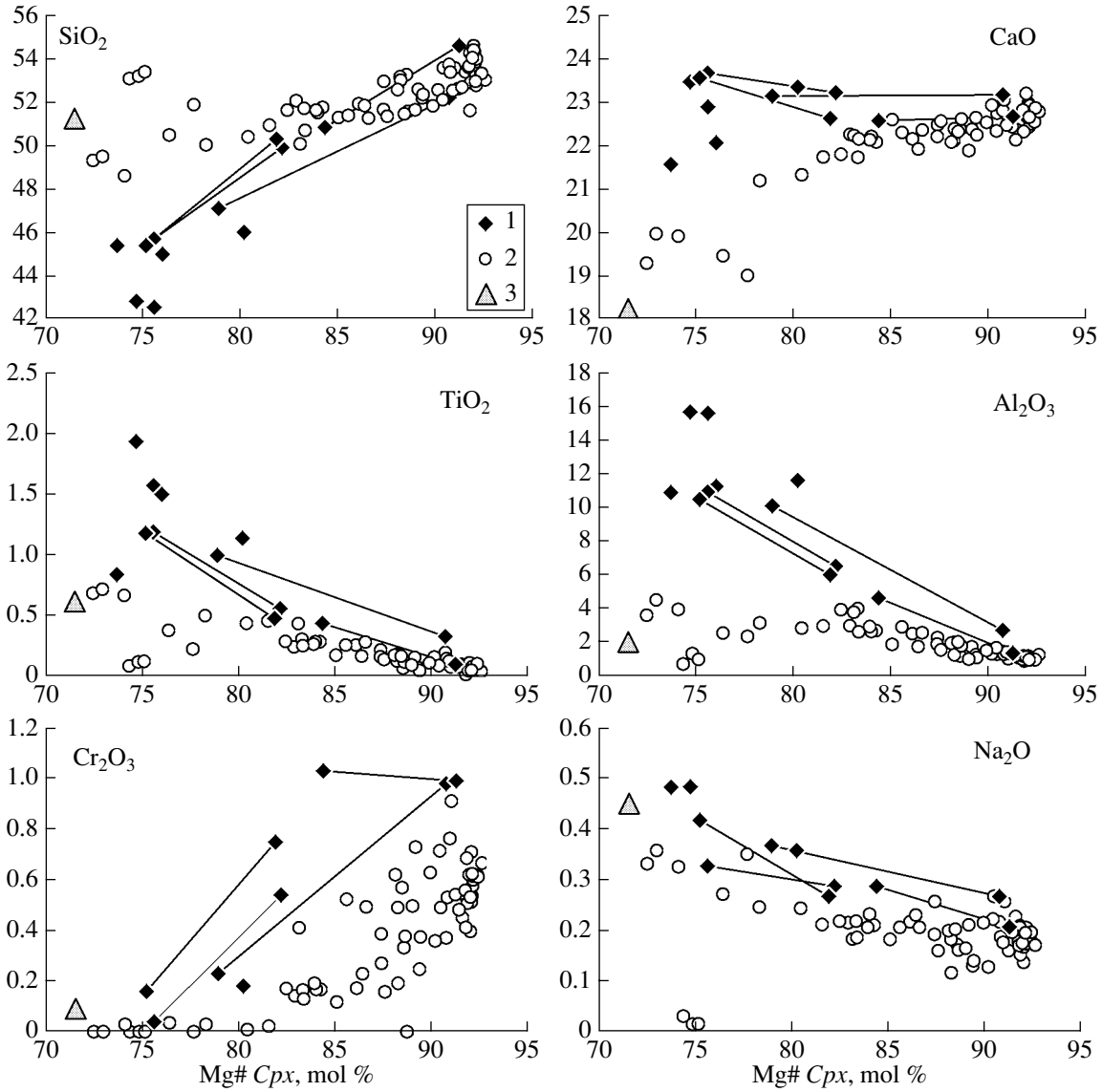

Fig. 3. Composition (wt %) of daughter pyroxene in melt inclusions.
(1) Daughter pyroxene in partly recrystallized melt inclusions; (2) pyroxene phenocrysts in avachites; (3) average composition of pyroxene in the avachite groundmass (Portnyagin *et al.*, 2005). Lines connect the composition points of the cores (more magnesian) and rims (more ferrous) of daughter pyroxene crystals.

nopyroxene and spinel crystals are unusually aluminous, the spinel and residual glasses are highly magnesian. The daughter phases of the inclusions are principally different from the phenocrysts in the rocks and include no plagioclase. Similar compositional features of daughter minerals in melt inclusions are typical of many arc and within-plate lavas (see, for example, Della-Pasqua *et al.*, 1995). A noteworthy feature of melt inclusions in high-Mg olivine from avachites is the occurrence of their daughter phases in the form of large single crystals (Fig. 1a–1c). Inclusions with a microlitic texture were found exclusively in ferrous olivine with $Fo < 87$ mol %.

Melt inclusions in avachites are commonly surrounded by halos of tiny secondary inclusions (Fig. 1b), which are restricted to the [001] plane of the host olivine. These aureoles are absent only from around the finely recrystallized inclusions in the ferrous olivine (Fig. 1d). The occurrence of halos of secondary inclusions suggests that the inclusions were reopened after their capture by olivine (Roedder, 1984). Some of these aureoles are very broad (stretch for as much as hundreds of micrometers away from the parent inclusion) and consist of large (up to 10 μm) melt and fluid inclusions (Fig. 1f). The primary inclusions themselves bear unusually large gas bubbles (up to 50% by volume) and little glass. The secondary inclusions are, conversely,

mostly vitreous and contain a small gas bubble. Other halos are not as broad and are made up of submicrometer-sized inclusions that occur within a distance of no more than 10–20 μm from the primary inclusion. Inclusions in olivine from avachites can be surrounded by various halos, which "document" the various degrees of decrepitation of these inclusions.

5. COMPOSITION OF HOMOGENIZED INCLUSIONS

5.1. Major Elements

The recrystallized melt inclusions were homogenized experimentally following the technique described in Section 3.1. Upon their quenching, the inclusions contained glass, a fluid bubble, and, sometimes, single spinel crystals and a sulfide phase (Fig. 1g–1i). A halo of tiny secondary inclusions around the primary ones was left after the experiments without any visible transformations. We did not examine experimentally the obviously reopened inclusions with wide halos of large inclusions. The compositions of glasses of the melt inclusions are listed in Table 3 and plotted in Fig. 5.

The compositions of the inclusions show broad variations in the contents of major components. The contents of Al_2O_3 (12.7–18.5 wt %) and Na_2O (2.2–4.7 wt %) are correlated negatively with the Mg# of the host olivine ($Fo_{85.8–90.7}$), and the MgO contents in the glass (8.0–15.8 wt %) are correlated positively with this parameter. The variations in the concentrations of SiO_2 (47.0–55.2 wt %) and CaO (8.9–15.6 wt %) are extremely broad at the relatively narrow range of the compositions of the host olivine and display only weak, statistically insignificant tendencies toward a decrease (for SiO_2) and increase (for CaO) with increasing Mg# of the olivine. The contents of FeO* (4.4–7.0 wt %), K_2O (0.4–1.0 wt %), TiO_2 (0.5–1.4 wt %), and P_2O_5 (0.13–0.38 wt %) are not correlated with the olivine composition. Some inclusions in the most magnesian olivine ($Fo_{>89}$) are close to avachites and their possible parental melt AV-91 (Portnyagin *et al.*, 2005) in the contents of MgO, Al_2O_3, Na_2O, K_2O, TiO_2, and P_2O_5 but have higher CaO and lower SiO_2 and FeO* concentrations. Inclusions in the relatively ferrous olivine ($Fo_{<89}$) display only partial correspondence to the compositions of the primitive basalts of Avachinsky volcano, and many of these inclusions are characterized by lower contents of SiO_2 and higher CaO, Na_2O, TiO_2, K_2O, and P_2O_5 concentrations. The FeO* contents of all of the inclusions are systematically lower than in the rocks.

As can be seen in Figs. 6a and 6b, the contents of TiO_2, K_2O, and P_2O_5 are positively correlated with one another and are significantly higher than the corresponding concentrations in the rocks. At the same time, the SiO_2 contents in the melt inclusions are negatively correlated with the CaO contents and positively with Na_2O (Figs. 6c, 6d). In this systematics, the compositions of the inclusions are much more alkaline and calcic than the compositions of the rocks. The two groups of the mutual correlations of the compositions of the inclusions are independent: the high-K group of the inclusions comprises compositions with different SiO_2 concentrations.

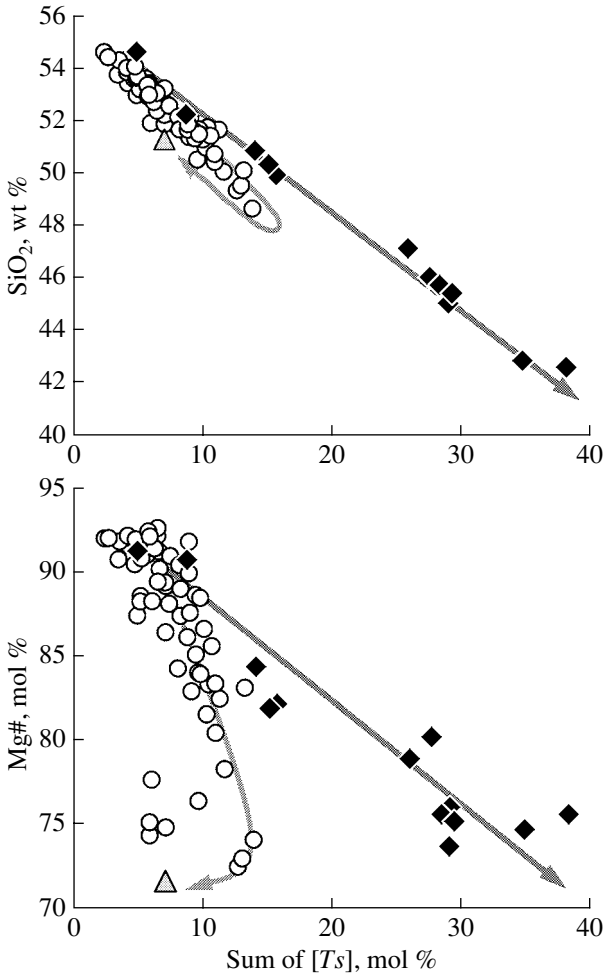

Fig. 4. Variations in the sum of tschermakite end members [*Ts*] in the daughter pyroxene of melt inclusions.
See Fig. 3 for symbol explanations. Arrows correspond to the evolutionary compositional trends of pyroxene in melt inclusions and rocks.

5.2. Volatile Components (H_2O, S, and Cl)

The H_2O concentrations in the melt inclusions, which were evaluated from the analytical totals of major oxides, ranged within the errors of microprobe analyses and did not exceed 0.1–0.3 wt %. The H_2O concentrations measured on an ion microprobe in two inclusions did not exceed the background values (~0.1 wt % on the day when the analyses were conducted). An independent criterion for the evaluation of the water content in the melt can be the difference between the calculated "dry" and the actual quenching

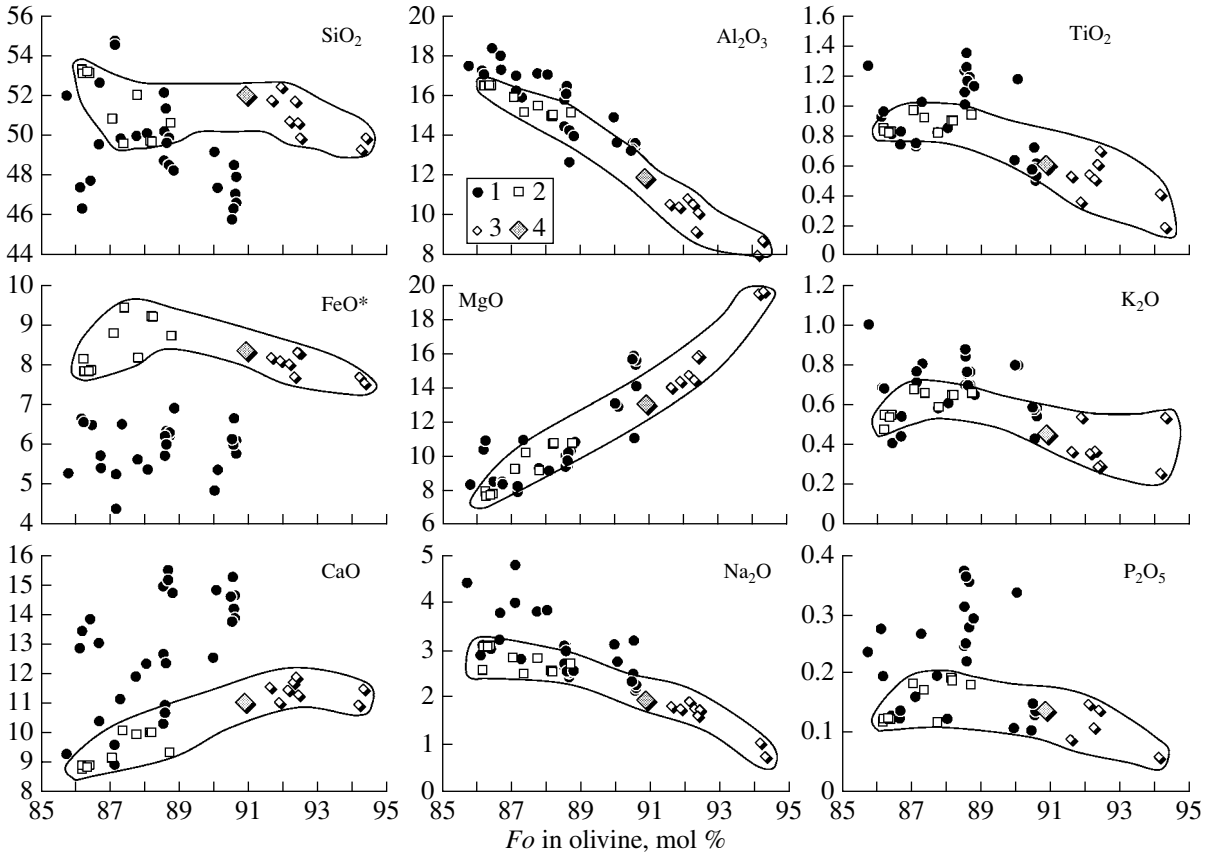

Fig. 5. Major-element concentrations (wt %) in homogenized melt inclusions as functions of the host-olivine composition. (1) Melt inclusions; (2) magnesian basalts of Avachinsky volcano (Castellana, 1998); (3) avachites; (4) calculated parental melt of avachites AV-91 (Portnyagin *et al.*, 2005). Fields correspond to the compositional fields of rocks (avachites and magnesian basalts) from Avachinsky volcano. The composition of olivine in equilibrium with the bulk-rock compositions is calculated by the model from (Ford *et al.*, 1983) at $Fe^{2+}/Fe^{3+} = 7$ in the melt.

temperatures of the inclusions (Sobolev *et al.*, 1989). The similar values of these temperatures for inclusions in olivine from avachites (Table 3, Fig. 7) testify to very low water content in the melt, no more than 0.5 wt %. The evaluations of the water concentrations in an avachite melt conducted in (Matveev *et al.*, 2005) on the basis of the hydrogen concentration in the olivine phenocrysts (IR spectroscopic analyses) yield 0.5 ± 0.1 wt %.

The Cl concentrations in the inclusions (0.08–0.15 wt %) slightly increase as the Mg# of the host olivine decreases and reveal a strong positive correlation with the Na_2O concentration (Figs. 8a, 8b). There is no correlation between the contents of Cl and K_2O, and the ratio of these components $Cl/K_2O = 0.1–0.3$ varies independently on the composition of the host olivine.

The maximum S concentration (up to 0.21 wt %) were found in inclusions captured by the most magnesian olivine ($Fo_{>89}$). The S contents in other inclusions are somewhat lower (0.06–0.12 wt %) and are not correlated with the composition of the olivine (Fig. 8c, 8d). Strong correlations were detected between the S and MgO contents and between the former and the quenching temperature of the inclusions. The S and Cl concentrations show weak negative correlations, and the S/Cl ratio (equal to 0.5–2.3) is positively correlated with the Mg# of the olivine. Inclusions in the relatively ferrous olivine show a strong positive correlation between the S and FeO* contents, perhaps, due to equilibrium between the melt in the inclusions and the daughter sulfide phase (Danyushevsky *et al.*, 2002a) and because of the incomplete melting of the sulfide during the experiment.

5.3. Trace Elements

All inclusions display trace-element patterns typical of arc magmas (Fig. 9). The distinctive geochemical features of the inclusions are their low contents of HREE and Y as compared with MORB; enrichment in LREE relative to HREE ($La_N/Yb_N = 1.5–4.2$); deep minima at the normalized Nb contents relative to LREE, K, and Th; and significant enrichment in LILE (Ba, K, and Sr), as well as in B and Cl. The HREE and Y contents are similar in all of the inclusions. MREE

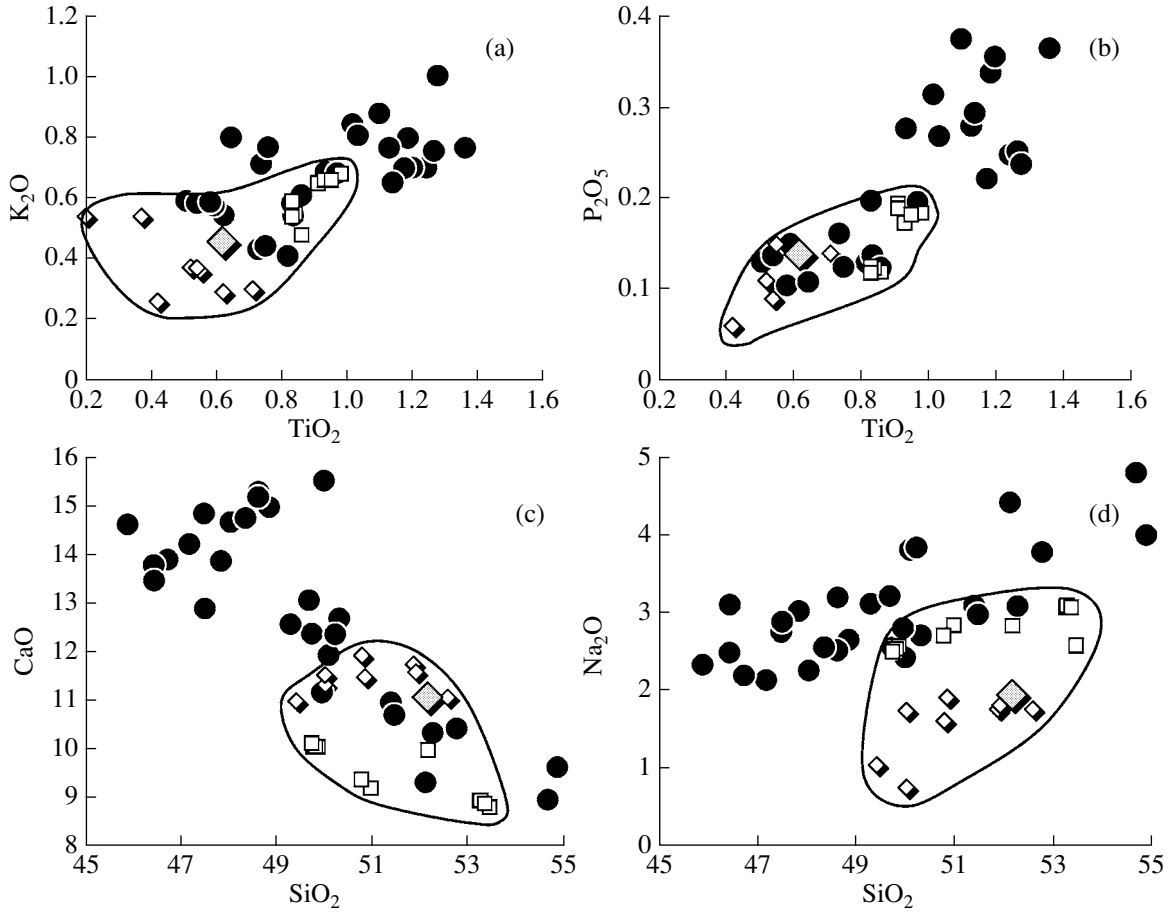

Fig. 6. Major-element concentrations (wt %) in homogenized melt inclusions.
See Fig. 5 for symbol explanations.

and more incompatible elements exhibit variations by factors of 2–4, which exceed the analytical errors and indicate that the compositions of the primitive melts of avachites had strongly varying contents of incompatible elements (Table 4). The melts rich in K, P, and Ti (Figs. 6a, 6b) are also most strongly enriched in LREE, Sr, Ba, Nb, and Th. The systematics of light trace elements (B, Be, and Li) is unusual. Their concentrations are positively correlated with one another, negatively with the Mg# of the olivine and the MgO contents of the melts, and negatively with Na_2O and volatile components (Cl and S) in the melts. The parental melt of avachites AV-91, whose composition was evaluated in (Portnyagin *et al.*, 2005) based on the composition of the rocks, is close to the composition of the inclusions most depleted in trace elements (Fig. 9).

6. OLIVINE COMPOSITION AROUND MELT INCLUSIONS

The detailed analysis of olivine zoning at the boundary with melt inclusions is important for evaluating the possible reequilibration of inclusions with this olivine after the capture of the inclusions (Danyushevsky *et al.*, 2000) and for identifying foreign melts that were not in equilibrium with this olivine when captured by the mineral (Danyushevsky *et al.*, 2003). This paper reports the results of our detailed study of three large (~100 μm) inclusions and their host olivines: magnesian ($Fo_{90.1–90.7}$, inclusions 2a and 3, Table 3) and more ferrous ($Fo_{86.4}$, inclusion 10a, Table 3). The composition of the olivine was examined by microprobe profiling over a length of 40 μm away from the melt inclusion. For each inclusion, two microprobe profiles were run in two perpendicular directions with analytical spots spaced 2 μm apart. The results of this study are presented in Fig. 10.

The comparison of two discrete profiles for each of the inclusions demonstrates their remarkable similarities (within the analytical accuracy) and suggests the existence of a concentric zoning in the host olivine around the inclusions. The zoning around inclusions in the high-Mg olivine is expressed as narrow (~5 μm) zones of more magnesian olivine adjacent to the melt inclusions. The CaO and NiO contents in this zone are analogous to those in the olivine away from the inclusion. Olivine around inclusion 10a exhibits broader compositional variations. A gradual increase in the

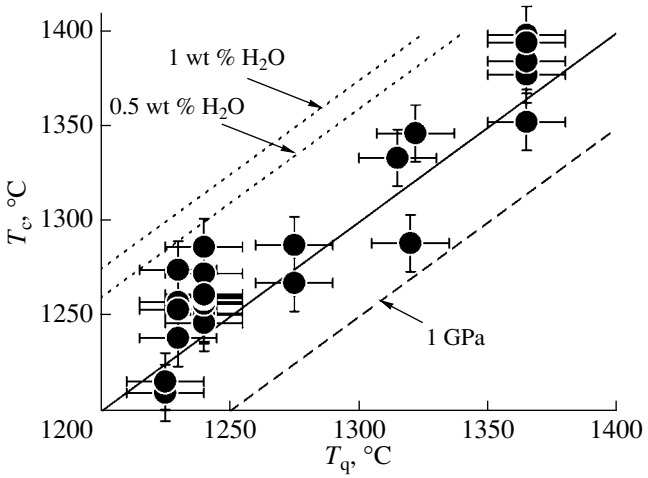

Fig. 7. Correlations between the experimental quenching temperatures of melt inclusions (T_q) and their pseudoliquidus temperatures (T_c) calculated by the model from (Ford *et al.*, 1983) at 1 atm pressure.

Dotted lines correspond to the expected difference between these temperatures at a water content of 0.5 and 1 wt % in the melt (Falloon and Danyushevsky, 2000). The dashed line corresponds to a pressure of 1 GPa (10 kbar) at a liquidus slope of 5°C/kbar (Danyushevsky *et al.*, 1996).

Mg# of this olivine (from Fo_{85} to $Fo_{86.5}$) occurs over a distance of 20 μm from the contact with the inclusion, after which the Mg# of the olivine remains practically unchanged. Olivine in contact with the inclusion is strongly enriched in CaO (0.35–0.50 wt %) and slightly depleted in NiO (~0.20 wt %) relative to olivine away from the inclusion (CaO = 0.2 wt %, NiO = 0.25 wt %).

Profiles near the inclusions intersected the decripitation halos around them but did not reveal any systematic variations in the composition of the olivine. It is also important to mention that the olivine crystal containing inclusion 10a is zonal, with the olivine zoning around the inclusion overprinted on the preexisting olivine zoning and being not related to it. This fact indicates that diffusion zoning in olivine around the inclusions developed under the effect of younger processes, after the capture of the inclusions by olivine.

7. DISCUSSION

7.1. Melt Inclusions versus *True Magmatic Liquids*

It is now admitted by most researchers that primary melt inclusions in minerals were formed by portions of the ambient melt captured by growing crystals. In interpreting the compositions of the inclusions, the follow-

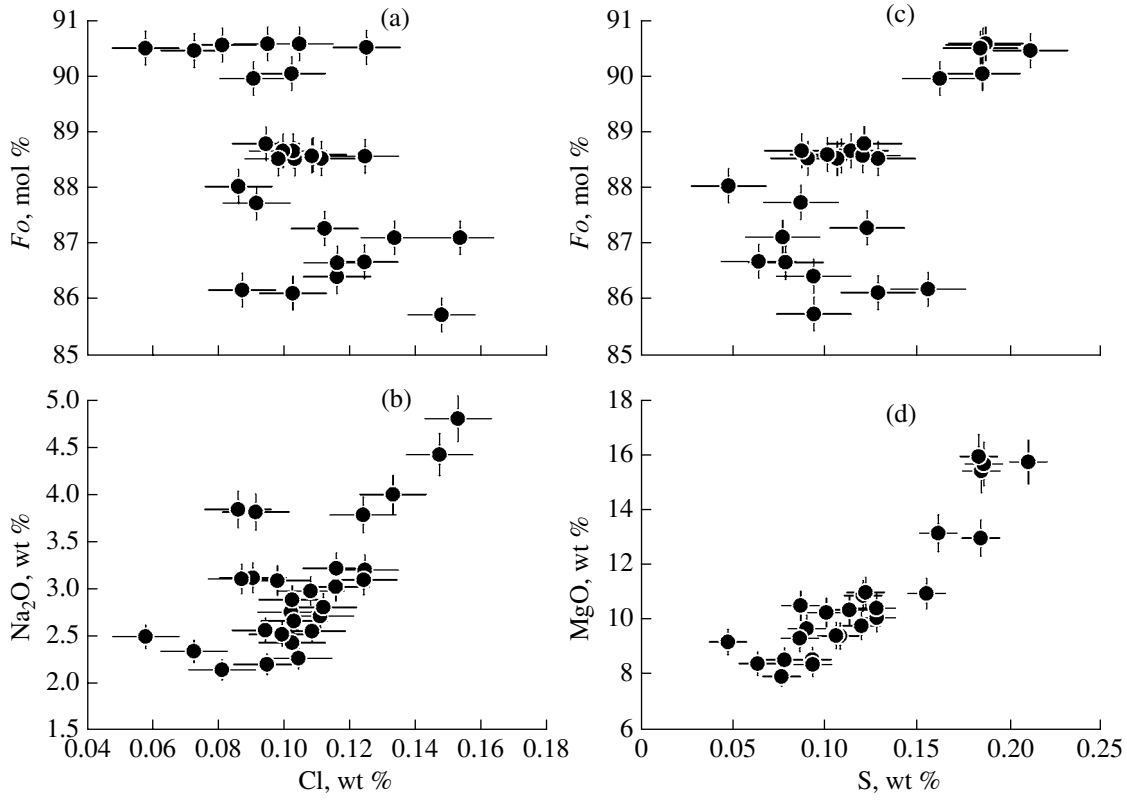

Fig. 8. Variations in the concentrations of S and Cl in melt inclusions as functions of the host-olivine composition and the concentrations of major oxides in inclusions.

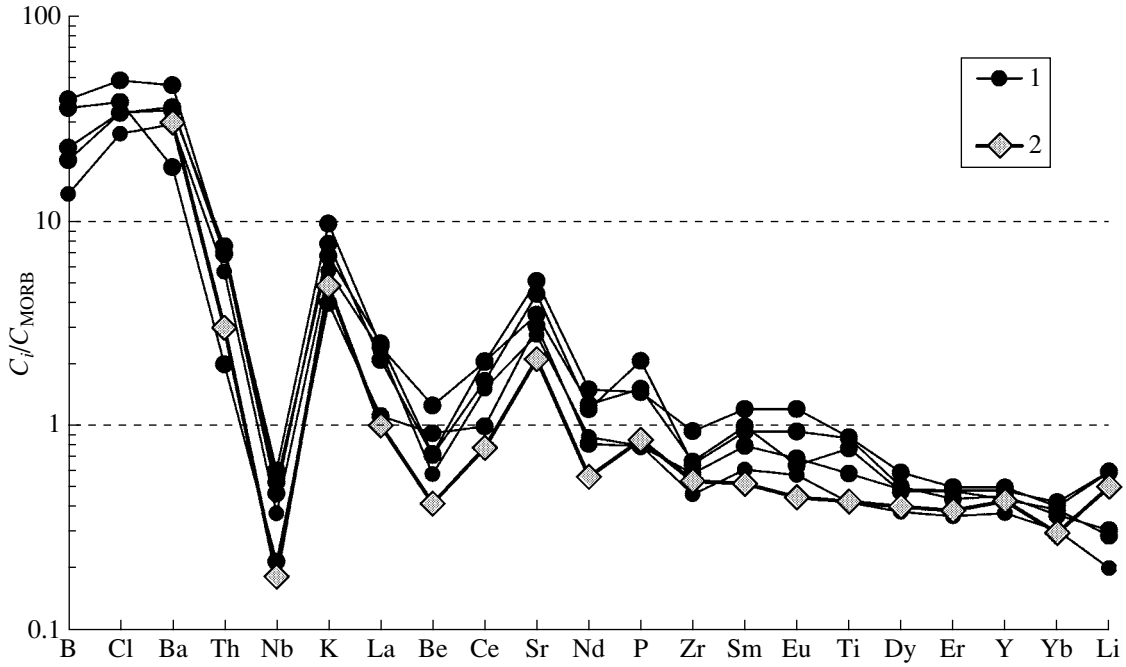

Fig. 9. N-MORB (Hofmann, 1998; *EarthRef*, 2004) normalized trace-element patterns for (1) melt inclusions and (2) the parental melt of avachites (Portnyagin *et al.*, 2005).

ing problems are pivoting: (i) how representative were such inclusions as samples of large magma volumes during their capture, and (ii) how significantly were (or were not) their compositions modified after the capture. Different aspects of these problems were extensively discussed in the literature (Roedder, 1984; Qin *et al.*, 1992; Tait, 1992; Gaetani and Watson, 2000; Danyushevsky *et al.*, 2000, 2002a, 2002b, 2003, 2005).

The key problem in considering the interpretation of melt inclusions as samples of the mineralizing medium stems from the fact that, because of their small sizes, inclusions can consist of a melt captured by the crystal from within its growth front, and this melt can have a composition different from that of the melt away from the crystal. This problem is referred in the literature to as the capture of inclusions from the boundary layer (Roedder, 1984). The reasons for the development of this layer, as well as its characteristic sizes and properties, are beyond the scope of our paper. It is important to stress the following points: if the composition of the boundary layer is characterized by depletion in the components of the growing crystal alone (olivine in the context of this research), this does not complicate any significantly the interpretation of melt inclusions. Techniques of the mathematical simulations of magma crystallization (see, for example, Danyushevsky *et al.*, 2002a) make it possible to reproduce the composition of the melt that was in thermodynamic equilibrium with the olivine at any moment of its crystallization. A more serious problem is the capture of the boundary layer melt differentiated in terms of elements incompatible to the host mineral (such as Ca, Al, Ti, and Na) (Kuzmin and Sobolev, 2003). The quantitative simulation of this process is a task for forthcoming investigations and should relay on the knowledge of mutually consistent diffusion coefficients of different components under various conditions, the growth rates of the crystals, and the efficiency of convective mass transfer. However, the practical approach to the solution of the problem of possible inclusion capture from the boundary layer is quite obvious. This approach is based on revealing correlations between the sizes of the inclusions and their composition in terms of components incompatible to olivine: the smaller the melt inclusion, the higher its contents of boundary-layer components. We conducted such a test for the inclusions discussed in this paper and revealed no correlations between the sizes of these inclusions and the contents of any melt components or their ratios. This result implies that the widths of the boundary layers around crystals should have been certainly smaller than the radii of the smallest of the inclusions (<10 μm), or the composition of the boundary layer did not differ (within the microprobe analysis accuracy) from the melt composition away from the crystal. By virtue of these data, we arrived at the conclusion that the capture of the boundary layer material could not cause the compositional diversity of the inclusions and their differences from the compositions of the rocks.

Isolated by its host crystal from the mineralizing medium, a melt inclusion continues to evolve in response to changes in the external conditions and can exchange material with its host mineral and the magma around it, as well as becomes partly or fully recrystal-

Table 3. Composition (wt %) of partly homogenized melt inclusions in olivine

Component	1	2a	2b	2c	2d	2e	3	4a	4b	4c	4d	4e	4g	4i	4j
	Melt inclusions														
SiO_2	47.95	47.36	47.03	47.36	46.16	45.88	47.88	49.03	51.68	50.49	50.21	48.87	52.21	49.92	51.84
TiO_2	0.72	0.51	0.54	0.61	0.59	0.58	1.20	1.25	1.27	1.02	1.13	1.20	1.10	1.18	1.37
Al_2O_3	13.46	13.43	13.52	13.43	13.26	13.24	13.79	14.53	16.11	16.35	12.73	14.35	15.81	16.57	16.23
FeO*	6.61	5.84	6.19	5.73	6.00	6.18	5.46	6.29	6.42	5.79	6.29	6.38	6.25	6.08	6.09
MnO	0.10	0.09	0.10	0.14	0.08	0.14	0.08	0.11	0.12	0.11	0.09	0.11	0.12	0.10	0.10
MgO	10.99	15.49	15.78	13.97	15.85	15.74	13.10	10.15	9.51	9.76	10.60	10.46	9.46	10.34	9.90
CaO	15.10	14.30	14.01	14.48	13.72	14.64	14.99	15.06	11.04	12.75	15.62	15.29	10.34	12.44	10.80
Na_2O	3.16	2.15	2.22	2.24	2.48	2.34	2.78	2.67	3.12	2.72	2.44	2.54	3.09	2.57	3.00
K_2O	0.43	0.59	0.59	0.54	0.57	0.59	0.80	0.70	0.76	0.85	0.77	0.70	0.88	0.70	0.77
P_2O_5	n.a.	0.13	0.14	n.a.	0.15	0.10	0.34	0.25	0.25	0.32	0.28	0.36	0.38	0.22	0.37
Cl	0.12	0.08	0.10	0.10	0.06	0.07	0.10	0.10	0.13	0.11	0.10	0.10	0.10	0.11	0.11
S	n.a.	0.19	0.19	n.a.	0.18	0.21	0.19	0.13	0.11	0.09	0.09	0.11	0.11	0.10	0.12
Cr_2O_3	n.a.	0.25	0.27	n.a.	0.32	0.27	0.14	0.14	0.07	0.03	0.11	0.08	0.07	0.06	0.05
Total	98.63	100.41	100.67	98.61	99.43	100.00	100.84	100.39	100.59	100.37	100.46	100.53	99.91	100.38	100.76
	Host olivine														
SiO_2	41.02	41.19	40.88	40.88	39.56	40.04	40.88	40.65	40.77	40.44	40.77	40.46	40.83	40.78	40.80
FeO*	9.29	9.29	9.21	9.21	9.24	9.34	9.71	11.13	11.12	11.08	11.02	11.03	11.15	11.17	11.11
MnO	0.16	0.14	0.16	0.16	0.15	0.18	0.17	0.20	0.19	0.17	0.21	0.20	0.19	0.19	0.19
MgO	49.85	50.04	49.78	49.78	49.50	49.78	49.36	48.22	48.40	48.02	48.41	48.45	48.30	48.74	48.37
CaO	0.16	0.17	0.17	0.17	0.17	0.19	0.19	0.19	0.23	0.25	0.16	0.25	0.21	0.23	0.21
NiO	0.19	0.17	0.16	0.16	0.18	0.15	0.17	0.15	0.16	0.18	0.16	0.16	0.17	0.16	0.16
Cr_2O_3	0.07	0.00	0.03	0.03	0.03	0.02	0.03	0.03	0.00	0.00	0.00	0.01	0.01	0.04	0.00
Total	100.73	101.00	100.39	100.39	98.84	99.70	100.51	100.56	100.87	100.14	100.73	100.55	100.85	101.32	100.84
Fo, mol %	90.5	90.6	90.6	90.6	90.5	90.5	90.1	88.5	88.6	88.5	88.7	88.7	88.5	88.6	88.6
∅, μm	n.a.	100	60	n.a.	75	50	100	50	15	40	40	50	30	30	15
T_q, °C	1320	1365	1365	1365	1365	1365	1315	1240	1240	1240	1240	1240	1240	1240	1240
T_c, °C	1289	1378	1385	1353	1399	1395	1334	1251	1252	1247	1262	1258	1257	1260	1261

Table 3. (Contd.)

Component	4k	4l	5	10a	10b	11a	11b	12a	12b	12c	12d	12e	14	*	**	***
	Melt inclusions													Glass standard		
SiO_2	48.68	50.15	50.42	48.12	50.13	47.73	46.17	53.13	55.20	53.95	49.88	48.46	52.51	51.01	0.03	50.81
TiO_2	1.15	1.04	0.66	0.82	0.76	0.94	0.96	0.84	0.74	0.75	0.85	0.80	1.29	1.83	0.02	1.85
Al_2O_3	14.08	16.01	15.28	18.53	18.21	17.38	17.00	17.46	16.37	16.82	16.97	16.59	17.67	14.14	0.01	14.06
FeO*	7.00	6.58	5.00	6.58	5.82	6.73	6.56	5.49	5.33	4.37	5.38	5.49	5.37	11.73	0.01	11.94
MnO	0.08	0.14	0.10	0.11	0.13	0.09	0.11	0.05	0.11	0.10	0.07	0.15	0.10	0.20	0.01	0.22
MgO	10.99	11.08	13.47	8.66	8.67	10.52	10.93	8.51	8.03	8.22	9.17	9.07	8.49	6.83	0.03	6.71
CaO	14.87	11.23	12.88	13.97	13.20	12.97	13.40	10.51	9.70	8.85	12.29	11.56	9.40	11.14	0.08	11.12
Na_2O	2.58	2.82	3.19	3.05	3.25	2.90	3.09	3.81	4.03	4.74	3.82	3.69	4.46	2.62	0.05	2.62
K_2O	0.66	0.81	0.82	0.41	0.45	0.69	0.68	0.55	0.72	0.76	0.60	0.56	1.01	0.19	0.19	0.19
P_2O_5	0.30	0.27	0.11	0.13	0.13	0.28	0.20	0.14	0.16	n.a.	0.12	0.19	0.24	0.22	0.02	0.20
Cl	0.10	0.11	0.09	0.12	0.12	0.10	0.10	0.13	0.13	0.15	0.09	0.09	0.15	0.02	0.01	
S	0.12	0.12	0.16	0.09	0.08	0.13	0.15	0.06	0.08	n.a.	0.09	0.05	0.09	0.14	0.05	0.14
Cr_2O_3	0.10	0.07	0.12	0.03	0.01	0.06	0.10	0.04	0.03	n.a.	0.02	0.03	0.02	0.03	0.05	
Total	100.70	100.41	102.31	100.60	100.92	100.49	99.46	100.72	100.62	98.70	99.36	96.74	100.78	100.10		99.86
	Host olivine													Olivine standard		
SiO_2	40.75	40.60	40.88	39.66	40.25	40.18	38.75	40.49	40.43	40.43	39.41	40.35	40.08	40.83	0.18	40.81
FeO*	10.91	12.31	9.96	12.99	12.89	13.35	13.30	12.81	12.44	12.44	11.88	11.78	13.63	9.59	0.10	9.55
MnO	0.18	0.21	0.17	0.22	0.19	0.22	0.22	0.20	0.20	0.20	0.22	0.21	0.21	0.15	0.02	0.14
MgO	48.56	47.45	50.12	46.43	47.03	46.53	46.60	46.82	47.23	47.23	47.76	48.68	45.99	49.37	0.32	49.42
CaO	0.17	0.24	0.19	0.18	0.23	0.20	0.19	0.22	0.21	0.21	0.20	0.21	0.19	0.10	0.00	<0.05
NiO	0.18	0.20	0.23	0.24	0.25	0.10	0.12	0.22	0.18	0.18	0.13	0.16	0.17	0.36	0.02	0.37
Cr_2O_3	0.01	0.01	0.03	0.02	0.02	0.00	0.01	0.04	0.01	0.01	0.02	0.02	0.01	0.01	0.01	
Total	100.76	101.02	101.58	99.74	100.85	100.57	99.18	100.79	100.67	100.67	99.62	101.40	100.27	100.40		100.29
Fo, mol %	88.8	87.3	90.0	86.4	86.7	86.1	86.2	86.7	87.1	87.1	87.8	88.1	85.8	90.2	0.06	90.2
∅, μm	30	50	70	100	n.a.	n.a.	50	30	20	n.a.	50	50	40			
T_q, °C	1240	1240	1322	1225	1225	1275	1275	1230	1230	1230	1230	1230	1240			
T_c, °C	1273	1287	1347	1210	1216	1268	1288	1239	1239	1275	1258	1254	1262			

Note: Numerals (1)–(14) correspond to the numbers of inclusions, ∅, μm is the diameter of the inclusions, T_q, °C is the quenching temperature of the inclusions, T_c, °C is the calculated pseudoliquidus temperature of the inclusions at 1 atm (Ford *et al.,* 1983), n.a.—means not analyzed. For standards: * is the average of the measured concentrations, ** is 1 σ, *** is the recommended concentration (Jarosewich *et al.*, 1980). Glass standard: USNM 111240/52 VG-2, four analyses; olivine standard: USNM 11312/44, six analyses.

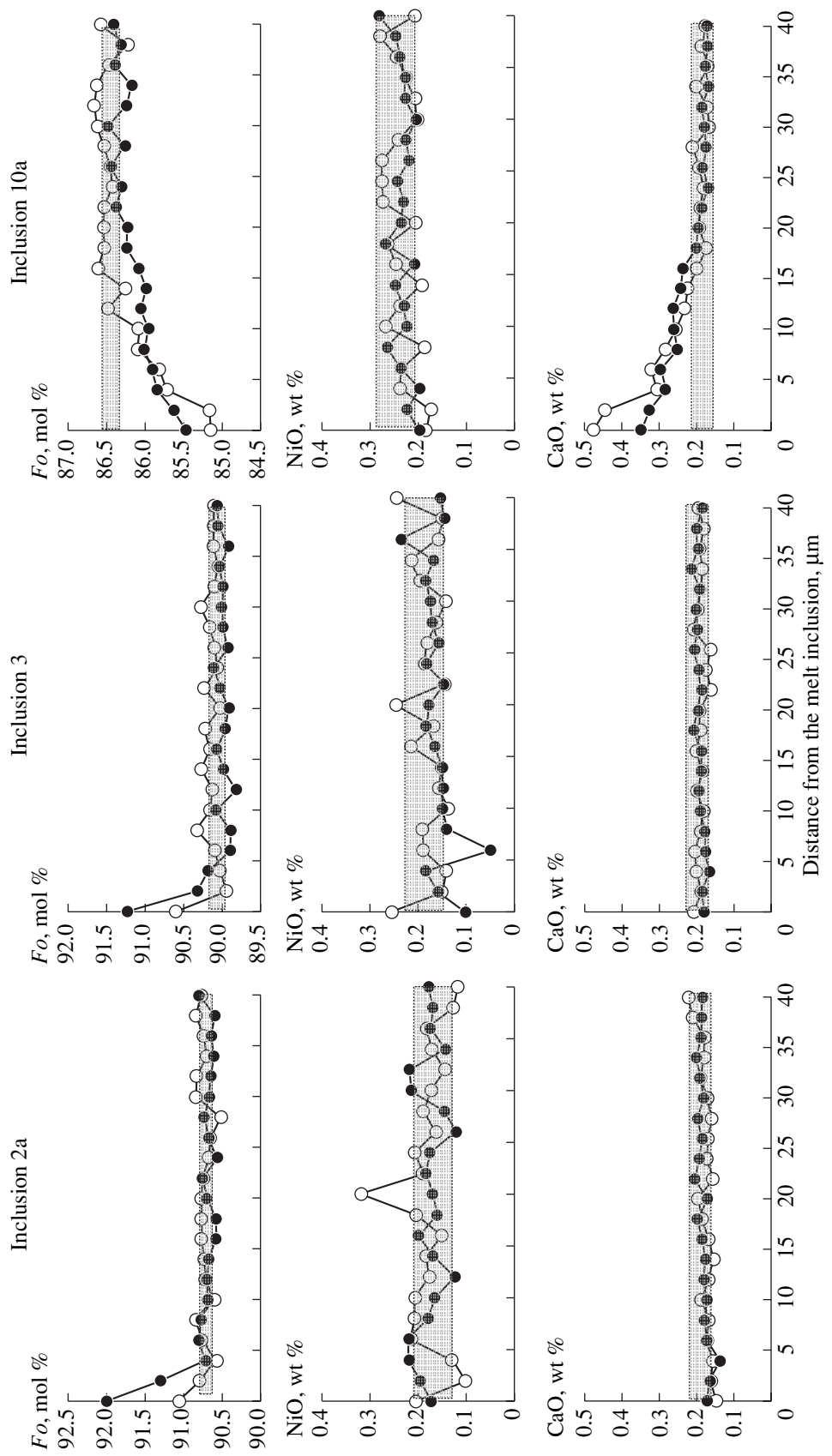

Fig. 10. Variations in the olivine composition near melt inclusions.
Solid and open circles demonstrate two microprobe profiles ran in two perpendicular directions for each inclusion. Shaded field denotes the host-olivine composition away from the melt inclusion.

lized. Below we consider in detail the effect of diffusion-controlled reequilibration, recrystallization, and decrepitation on the composition of melt inclusions in olivine from avachites.

7.2. Reequilibration of Inclusions with Their Host Olivine

Magma cooling caused avachite crystallization. An analogous process took place in the melt inclusions. In nature, the crystallization rate of magmas and the effective isolation of crystals from the ambient melt are such that minerals undergo partial diffusion-controlled reequilibration with the melt (Gaetani and Watson, 2000; Danyushevsky *et al.*, 2000). This process is one of the important reasons for differences between the evolutionary paths of the melt in the macrosystem and in inclusions. Inasmuch as the mass of the host mineral grain is much greater than the mass of a melt inclusion in it, the processes of their diffusion-controlled reequilibration occur in compliance with the laws of equilibrium with a mineral of constant composition, whereas in large magma volumes the melt, conversely, exerts the predominant effect on the composition of the crystals. The effect of crystallization and diffusion-controlled reequilibration is as follows: melt in an inclusion always has a Mg# equal to or higher than that of the ambient melt (Danyushevsky *et al.*, 2000). The effect of reequilibration of inclusions with olivine can be identified by the anomalously low Fe concentration in the homogenized melt inclusions and by the development of diffusion zoning in the olivine around the inclusion (if their reequilibration was not completed). As can be seen from Fig. 5, all inclusions in olivine contain 4.4–7.0 wt % FeO*. These values are systematically lower than the analogous contents in the rock (FeO* = 7.5–9.5 wt %). The zoning of olivine around the inclusions (Fig. 10) suggests that inclusions in high-Mg olivine were completely reequilibrated with the host olivine, whereas inclusions in the more ferrous olivine (which preserves its diffusion zoning) were partly reequilibrated. The reequilibration of the inclusions with the olivine also follows from the highly magnesian composition of daughter phases in the inclusions, as will be demonstrated below in Section 7.3.

The exchange of FeO and MgO between melt inclusions and olivine was discovered more than fifteen years ago (Gurenko *et al.*, 1988). A principal achievement of the past years is the possibility of the quantitative simulation of this process, which allows the researcher to evaluate the time needed for the reequilibration (Danyushevsky *et al.*, 2000, 2000b) and to obtain independent estimates for the temperature of the latest equilibrium between the melt and olivine and the initial FeO* concentration in the melt captured in the inclusion (Portnyagin and Hoernle, 2003). The results of simulation of the reequilibration between inclusions in avachites and olivine by the Fe-LOSS computer program (Danyushevsky *et al.*, 2002b) are presented in Fig. 11 and Table 5.

Table 4. Concentrations (ppm) of trace elements in melt inclusions

Element	1	2	3	4	5	6
	2a*	3	4a	10a	14a	AV-91
Li	1.22	1.87	1.75	3.62	3.59	3.1
Be	0.29	0.36	0.37	0.46	0.63	0.2
B	12.4	18.2	20.9	32.7	36.0	
Ti	3631	7479	6660	5009	7555	3660
Cr	1884	842	4086	87	196	
Sr	324	513	406	358	593	246
Y	14.0	16.9	16.3	18.0	18.6	16
Zr	44.7	63.0	64.9	56.6	91.4	52
Nb	1.14	1.43	1.62	0.66	1.85	0.56
Ba	248	300	289	153	385	253
La	7.64	6.89	8.32	3.66	8.00	3.3
Ce	14.9	16.3	20.4	9.78	20.2	7.7
Nd	8.46	11.5	12.2	7.81	14.4	5.4
Sm	2.11	3.24	3.43	2.76	4.17	1.8
Eu	0.77	1.26	0.86	0.93	1.63	0.6
Dy	2.26	3.01	2.85	2.92	3.53	2.4
Er	1.41	1.71	1.87	1.88	1.95	1.5
Yb	1.23	1.46	1.56	1.70	1.62	1.2
Th	0.94	1.15	1.26	0.33	1.16	0.5

Note: (1)–(5) compositions of inclusions; (6) is the parental avachite melt AV-91 (Portnyagin *et al.*, 2005). The concentrations of Li, Be, Dy, and Er in AV-91 are calculated from the composition of the liquidus pyroxene, other elements are calculated from the rock compositions; * are the numbers of inclusions.

The calculations conducted for inclusion 10a (the host olivine was $Fo_{86.4}$) indicate that the melt composition measured in the inclusion can be obtained if the initial melt with FeO* = 7.0 ± 0.5 wt % was captured in olivine $Fo_{86.4}$ at a temperature of 1135°C and was consequently cooled to ~1070°C. At this temperature, the inclusion was 65% reequilibrated with the host olivine for 45 days and was then quenched (for example, during magma eruption). The inclusion was homogenized experimentally at a temperature of ~1210°C. Note that the evaluated reequilibration temperature (1070°C) is quite close to the calculated liquidus temperature of the melt of the avachite groundmass (~1050°C, Table 1) and the equilibrium temperatures of the daughter phases (1109–1150°C, Section 4). The evaluated initial FeO* concentration in the melt (~7 wt %) appeared to be somewhat lower than that of avachites and the Mg-basalts of Avachinsky volcano (Fig. 5).

Analogous calculations made for inclusions 2a and 3 (whose host olivine was $Fo_{90.6}$ and $Fo_{90.1}$, respectively)

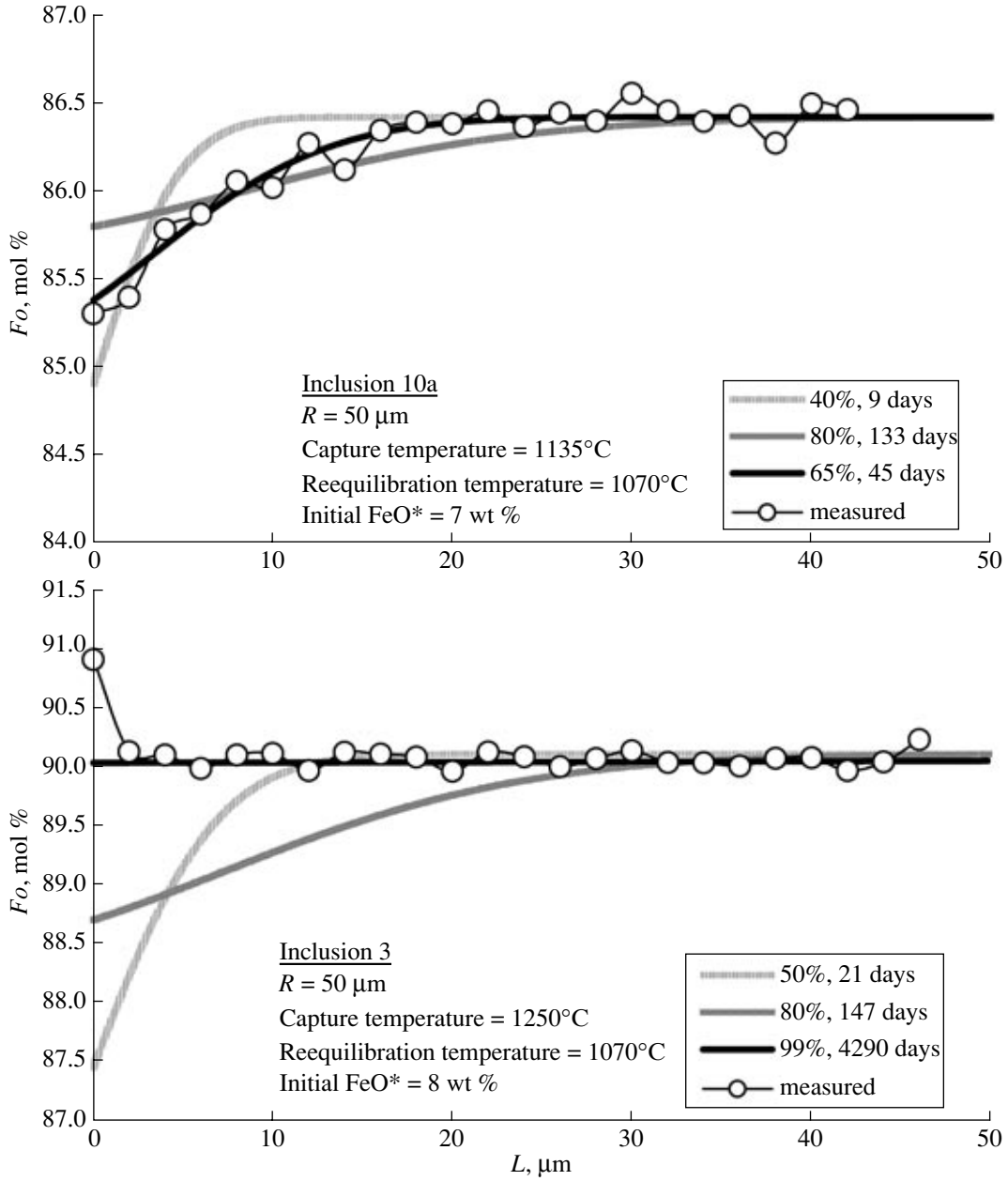

Fig. 11. Quantitatively simulated Fe and Mg diffusion profiles in olivine around melt inclusions. The profiles developed due to the reequilibration between the inclusions and host olivine.

L is the distance (μm) from the melt inclusion. Data are shown for an averaged olivine composition for two microprobe profiles for each of the inclusions (see Fig. 10).

demonstrate that the inclusions could be completely reequilibrated with the olivine at the same temperature of ~1070°C as the temperature for inclusion 10a, but the duration of this process should have been one order of magnitude longer, no less than 10 years. The initial FeO* concentration in the melts was evaluated at ~8 wt %, which is close to the composition of avachites. The anomalously high Mg# of the olivine in contact with melt inclusions 2a and 3 (Fig. 10) is explained by the brief time (20–30 min) of equilibrium between the olivine and high-Mg melt during the thermometric experiment on the homogenization of the inclusions (see Table 5 for the composition of olivine in equilibrium with the quenched melts).

The time of reequilibration between the inclusions and host olivine was evaluated for the equilibrium temperatures corresponding to anhydrous melts. In Sections 7.3 and 7.4 and in (Portnyagin *et al.*, 2005), it is mentioned that the probable initial H_2O concentrations in the melts were higher than 0.5 wt %, and the actual

Table 5. Results of quantitative simulation of the diffusion-controlled reequilibration of melt inclusions with their host olivine

Component	Inclusion 10a				Inclusion 3				Inclusion 2a			
	INIT[1]	RE-EQ	RE-HEAT	MEAS	INIT	RE-EQ	RE-HEAT	MEAS	INIT	RE-EQ	RE-HEAT	MEAS
SiO_2	48.07	48.60	47.83	47.88	47.24	48.94	47.50	47.58	47.3	49.13	47.29	47.26
TiO_2	0.85	0.89	0.81	0.82	1.22	1.44	1.18	1.19	0.55	0.66	0.51	0.51
Al_2O_3	19.23	20.21	18.39	18.44	14.07	16.59	13.62	13.70	14.48	17.34	13.43	13.40
Fe_2O_3	0.97	1.02	0.93	0.91	1.11	1.31	1.07	0.75	1.11	1.33	1.03	0.81
FeO	6.11	5.04	5.85	5.73	6.98	3.52	4.63	4.75	6.98	3.43	4.73	5.10
MnO	0.11	0.12	0.11	0.11	0.08	0.09	0.08	0.08	0.1	0.12	0.09	0.09
MgO	6.4	4.93	8.62	8.62	9.84	5.17	13.09	13.02	10.7	5.51	15.49	15.46
CaO	14.5	15.24	13.87	13.90	15.30	18.05	14.81	14.90	15.42	18.46	14.30	14.27
Na_2O	3.17	3.33	3.03	3.03	2.84	3.35	2.75	2.76	2.32	2.78	2.15	2.15
K_2O	0.43	0.45	0.41	0.41	0.82	0.97	0.79	0.79	0.64	0.77	0.59	0.59
P_2O_5	0.13	0.14	0.12	0.13	0.35	0.41	0.34	0.34	0.14	0.17	0.13	0.13
Cr_2O_3	0.03	0.03	0.03	0.03	0.14	0.17	0.14	0.14	0.27	0.32	0.25	0.25
FeO*	7.0	6.0	6.7	6.5	8.0	4.7	5.6	5.4	8.0	4.6	5.7	5.8
T, °C	1135	1070	1212	1212	1250	1070	1336	1336	1264	1074	1380	1380
Fo, mol %	86.4	85.3	90.2	90.4	90.1	90.0	95.0	94.9	90.7	90.6	95.6	95.3
Re-eq, %		65				99				99		
t, days		45				4290				4086		

Note: [1] Calculated and measured compositions of inclusions: INIT—initial composition of the melt captured by olivine, calculated by the technique from (Danyushevsky *et al.*, 2000); RE-EQ.—modeled composition of melt in the inclusion partly reequilibrated with the olivine, RE-HEAT—composition of the melt obtained by simulating the experimental homogenization of an inclusion partly reequilibrated with the olivine; MEAS—measured composition of the homogenized inclusion. Compositions of inclusions are normalized to 100%. FeO* is the total Fe in the form of FeO, *T*, °C is the temperature of reequilibration between the melt and olivine; *Fo*, mol % is the composition of olivine in equilibrium with melt in the inclusion, Re-eq, % is the extent of reequilibration between the melt and olivine calculated as the degree (in %) of approach of the Fe content in the melt to the Fe content in the melt completely equilibrated with the host olivine; *t*, days is the time needed for the melt to achieve the specified degree of reequilibration. Oxide contents are given in wt %.

liquidus temperatures of the melts were, perhaps, 60–100° lower (Falloon and Danyushevsky, 2000). A decease in the Mg and Fe diffusion rates with decreasing temperature should have required longer times for achieving the calculated degree of reequilibration between the inclusions and olivine. For example, the calculated reequilibration time for inclusion 10a was 45 days under anhydrous conditions, 108 days at a water content in the melt equal to 1 wt %, and 245 days at 2 wt % water. Of course, it is important to take into account the water contents for evaluating the reequilibration times, but this correction for the actual liquidus temperature does not principally modify the relations obtained in our simulations, namely, the reequilibration times of inclusions significantly differ for different crystals from the same avachite sample. On the one hand, this result can be interpreted as evidence for gradual cooling of the magmatic body. Magnesian olivine (grains 2 and 3) was the first to crystallize and occurred at magmatic temperatures for a longer time than later Fe richer olivine (grain 10). Then, the cooling rate can be evaluated at ~10°C/year. On the other hand, as was mentioned in Section 5, melt inclusions in avachites are variably enriched in incompatible elements. Inclusions 2a and 3, which are completely reequilibrated with olivine, are significantly enriched in LREE, Nb, and Th relative to the groundmass melt of avachites. Inclusion 10a is only partly reequilibrated, and its trace-element concentrations are close to those in the matrix melt (Fig. 9, Table 4), and, hence, the host olivine of this inclusion could have crystallized directly from the matrix melt of avachites shortly before the eruption. This observation led us to suggest that the assemblage of olivine phenocryst in avachites is hybrid. Its genesis should be related to at least two magmatic episodes, which were separated by a long-lasting interlude. During this interlude, some of the inclusions completely reequilibrated with the olivine. Inasmuch as the number of inclusions whose cooling histories were studied is small, this hypothesis cannot be regarded as validated reliably enough. Nevertheless, when considered together with independent data on the petrography of avachites, zoning of their minerals (Portnyagin *et al.*, 2005), and the geochemistry of the inclusions, our results serve as evidence in support of the hybrid and cumulative genesis of avachites.

Another outcome of our simulations is the evaluation of the initial FeO* concentrations in the melts,

Table 6. Initial composition (wt %) of melts inclusions

Component	1	2a	2b	2c	2d	2e	3	4a	4b	4c	4d	4e	4g	4i
SiO_2	48.34	47.31	46.99	47.92	46.69	46.14	47.24	48.56	50.88	49.70	49.73	48.38	51.66	49.34
TiO_2	0.73	0.55	0.59	0.65	0.66	0.65	1.22	1.25	1.23	0.99	1.13	1.20	1.07	1.17
Al_2O_3	13.57	14.51	14.81	14.25	14.87	14.79	14.07	14.49	15.62	15.89	12.73	14.36	15.38	16.37
FeO*	8.0	8.0	8.0	8.0	8.0	8.0	8.0	8.0	8.0	8.0	8.0	8.0	8.0	8.0
MnO	0.10	0.10	0.11	0.15	0.09	0.16	0.08	0.11	0.12	0.11	0.09	0.11	0.12	0.10
MgO	10.33	10.60	10.52	10.63	10.26	10.12	9.84	8.73	9.24	9.02	9.00	8.88	9.29	9.12
CaO	15.23	15.45	15.35	15.36	15.39	16.35	15.30	15.01	10.70	12.39	15.62	15.30	10.06	12.29
Na_2O	3.19	2.32	2.43	2.38	2.78	2.61	2.84	2.66	3.03	2.64	2.44	2.54	3.01	2.54
K_2O	0.43	0.64	0.65	0.57	0.64	0.66	0.82	0.70	0.74	0.83	0.77	0.70	0.86	0.69
P_2O_5		0.14	0.15		0.17	0.11	0.35	0.25	0.24	0.31	0.28	0.36	0.37	0.22
Cr_2O_3		0.27	0.30		0.36	0.30	0.14	0.14	0.07	0.03	0.11	0.08	0.07	0.06
Fo	90.5	90.6	90.6	90.6	90.5	90.5	90.1	88.5	88.6	88.5	88.7	88.7	88.5	88.6
P, GPa	0.6	0.7	0.7	0.6	0.7	0.6	0.6	0.2	1.0	0.7	–0.1	0.2	1.0	0.7
T_{1atm}	1267	1261	1261	1264	1259	1253	1250	1212	1246	1228	1218	1214	1252	1228
T_P	1299	1294	1297	1295	1296	1283	1280	1220	1295	1261	1214	1222	1304	1264
T_{P,H_2O}	1229	1224	1227	1225	1226	1213	1210	1150	1225	1191	1144	1152	1234	1194
Component	4j	4k	4l	5	10a	10b	11a	11b	12a	12b	12c	12d	12e	14
SiO_2	50.91	48.39	50.10	48.89	47.63	49.12	47.66	46.59	51.97	53.68	53.28	49.55	49.52	51.50
TiO_2	1.33	1.18	1.08	0.66	0.82	0.74	0.99	1.04	0.81	0.70	0.72	0.81	0.83	1.26
Al_2O_3	15.74	14.39	16.65	15.19	18.51	17.71	18.31	18.34	16.81	15.40	16.10	16.88	16.62	17.29
FeO*	8.0	8.0	8.0	8.0	8.0	8.0	8.0	8.0	8.0	8.0	8.1	8.0	8.0	8.0
MnO	0.10	0.08	0.15	0.10	0.11	0.13	0.09	0.12	0.05	0.10	0.10	0.15	0.07	0.10
MgO	9.28	8.94	8.12	10.07	7.28	7.63	7.08	6.96	7.78	8.20	7.91	8.22	8.34	6.94
CaO	10.47	15.20	11.68	12.80	13.96	12.83	13.66	14.46	10.12	9.13	8.47	11.76	12.04	9.20
Na_2O	2.91	2.64	2.93	3.17	3.05	3.16	3.05	3.33	3.67	3.79	4.54	3.75	3.74	4.36
K_2O	0.75	0.67	0.84	0.81	0.41	0.44	0.73	0.73	0.53	0.68	0.73	0.57	0.59	0.99
P_2O_5	0.36	0.31	0.28	0.11	0.13	0.13	0.29	0.22	0.13	0.15	0.00	0.19	0.12	0.23
Cr_2O_3	0.05	0.10	0.07	0.12	0.03	0.01	0.06	0.11	0.04	0.03	0.00	0.02	0.03	0.02
Fo	88.6	88.8	87.3	90.0	86.4	86.7	86.1	86.2	86.7	87.1	87.1	87.8	88.0	85.8
P, GPa	1.0	0.2	0.6	1.0	0.2	0.4	0.2	0.2	0.8	1.0	1.3	0.8	0.8	1.1
T_{1atm}	1246	1218	1208	1265	1168	1187	1165	1162	1217	1241	1251	1221	1224	1213
T_P	1297	1228	1239	1313	1179	1206	1177	1172	1258	1290	1314	1260	1262	1266
T_{P,H_2O}	1227	1158	1169	1243	1109	1136	1107	1102	1188	1220	1244	1190	1192	1196

Note: Numerals (1)–(14) correspond to the numbers of inclusions; the compositions of inclusions are recalculated to anhydrous residues and equilibrium with the host olivine (*Fo*) with an assumed FeO* content of 8 wt %, where FeO* is the total Fe in the form of FeO; *P*, GPa is the pressure of equilibrium between the melt and the olivine–clinopyroxene assemblage, calculated by the model (Danyushevsky *et al.*, 1996); T_{1atm}, °C is the temperature of equilibrium between the melt and olivine at 1 atm, calculated by the model (Ford *et al.*, 1983); T_P is the liquidus temperature of olivine at a calculated pressure (*P*); T_{P,H_2O} is the liquidus temperature of olivine at a calculated pressure and a water content in the melt equial to 1 wt %. The correction for a decrease in the liquidus temperature is introduced in compliance with (Falloon and Danyushevsky, 2000).

which was 7–8 wt % (Table 5) and was, within the accuracy of the calculations (±0.5 wt %), close to the values typical of the rocks themselves. Using these estimates, we recalculated all measured compositions of the inclusions to the primary equilibrium with the host olivine, assuming the initial FeO* = 8 wt % (Table 6). These recalculations significantly modified the contents of FeO* (which increased after the calculations), MgO, and SiO_2 (they decreased), while the concentrations of other melt components have changed insignificantly.

A noteworthy compositional characteristic of many inclusions from avachites is their high CaO contents (Fig. 5). Data on the diffusion zoning of olivine around inclusion 10a indicate that FeO and MgO in the inclusions were not the only components exchanging with the olivine, and CaO also participated in this process. The enrichment in CaO observed at the boundary of inclusion with olivine (Fig. 10) suggests that this component migrated from the inclusion to olivine. This process should have resulted in a decrease in the bulk CaO concentration in the inclusion, and cannot be responsible for the higher CaO concentration in the inclusions than in the rocks. For inclusion 10a, the correction for the decrease in the CaO content is less than 1 wt % and was neglected in the calculations. A possible explanation of CaO migration from the inclusions to their host mineral can be a significant increase in the distribution coefficient of this element between olivine and melt with decreasing temperature (Libourel, 1999).

7.3. Crystallization in Melt Inclusions

The recrystallization of melt inclusions is a widespread process in slowly cooling lavas and subvolcanic bodies. Although the compositions of the daughter phases of inclusions were reported in many publications (see, for example, Della-Pasqua *et al.*, 1995), the distinctive features of their compositions have never been described comprehensively. In this respect, avachites are convenient rocks, because the daughter phases of their inclusions occur as crystals large enough to be examined in much detail. The perfect crystal faceting of phases in many of the inclusions can be interpreted as caused by the entrapment of these minerals, together with the melt, in the form of crystals (Figs. 1a, 1c). However, the compositions of these crystals in inclusions notably differ from those of both the phenocryst minerals and the isolated crystalline inclusions of these minerals in olivine (Portnyagin *et al.*, 2005). The large sizes and euhedral habits of crystals contained in the inclusions leave no doubt that at least the marginal zones of these phases were in local equilibrium with the melt in the inclusions and did not result from rapid unequilibrated crystallization. Thus, the reason for the high-Al and high-Mg composition of the daughter phases can be either their growth from a melt of unusual composition or the unusual conditions of their crystallization, which existed only in the inclusions but not in the macrosystem as a whole.

Pyroxene and spinel grains contain cores whose composition is identical to those of the corresponding phenocrysts, which suggests that these minerals could be entrapped in inclusions together with melt and served as crystallization centers. It seems, however, hardly probable that pyroxene and spinel were simultaneously captured in an inclusion. It is more likely that the very early crystallization conditions in the inclusion and the composition of the inclusion itself did not differ from the crystallization conditions and the composition of the ambient magma where olivine, pyroxene, and spinel were also cotectic minerals (Portnyagin *et al.*, 2005). During the subsequent temperature decrease, the crystallization conditions in the microsystem of the melt inclusion deviated from those in the ambient magma, and this caused the unusual composition of the margins of daughter crystals in the inclusions. Although the liquidus minerals in the melt inclusions were the same as in the macrosystem, and the cooling regimes of both systems were identical, their crystallization conditions were different.

As can be seen in Fig. 4, the evolution of the pyroxene composition in the inclusions demonstrates similar trends to the compositional evolution of the phenocrysts. As the Mg# of the pyroxene decreases, it becomes enriched in the tschermakite component (in fact, the concentration of tetrahedrally coordinated Al increases). The crystallization in the inclusions differed from the whole rock, first, by an enhanced enrichment of the daughter pyroxene in the tschermakite component at given Mg# and, second, by a persistent increase in the Al content of the daughter pyroxene at low Mg#, whereas the Al content of the pyroxene phenocrysts starts to decline at some stage.

The former observation can be explained by the fact that a temperature decrease in melt inclusions triggers their reequilibration with the host olivine. In a situation with the fractional crystallization of olivine, the principal effect of this process is the maintenance of a constantly higher Mg# of melt in the inclusions than in the ambient melt (Danyushevsky *et al.*, 2000). Hence, at equal degrees of fractionation, which control the extent of Al enrichment in the melt, the liquidus pyroxene of the inclusion should have a composition equal to or more magnesian than the composition of the liquidus pyroxene in the ambient melt. This explains the steeper trend of Al enrichment in the pyroxene of the inclusions (Fig. 4b). Evidence that the inclusions did reequilibrate with the olivine is presented in Section 7.2.

A simple explanation of the compositional trend of the phenocrysts (Fig. 4a) is the appearance of plagioclase on the liquidus of the magma, with the crystallization of this mineral decreasing the Al content in the melt and, correspondingly, in the liquidus pyroxene. No plagioclase is present among the daughter phases of the melt inclusions, and this determines the extremely

strong Al enrichment (up to 24 wt %, Table 2) in the residual melt of the inclusions and the crystallization of pyroxene and spinel with unusually high Al contents. The reasons for the absence of plagioclase from the assemblage of the daughter phases remain not fully understood. It was demonstrated (Danyushevsky *et al.*, 2003) that the stable phase of melts oversaturated with plagioclase and occurring at temperatures above the liquidus of this mineral is spinel. The residual melts of the inclusions are of low-temperature nature and contain no water, judging from their analytical totals of major oxides (Table 2). In a dry system, plagioclase should be their liquidus phase (Danyushevsky *et al.*, 1996). A delay in the beginning of its crystallization could be caused by the former occurrence of significant water amounts (>5 wt %) in the residual melt. This water could be lost from the inclusions during later stages of their evolution. It can also be hypothesized that high-Al pyroxene and spinel were equilibrium but metastable phases of the inclusions. Their predominant (compared with plagioclase) crystallization could be controlled by kinetic factors that hampered plagioclase nucleation. Regardless of the reasons for plagioclase absence from among the daughter phases of the inclusions, a principally important result of our research is the identification of the differences between the crystallization conditions in the melt inclusions and the melt around olivine grains. These differences explain the origin of unusual high-Al phases in the inclusions in the absence of high-Al magmas, in contrast to what was proposed previously in (Della-Pasqua *et al.*, 1995).

7.4. Decrepitation of Melt Inclusions

The decrepitation of inclusions in minerals or, in other words, the reopening of these inclusions is a widespread consequence of magma decompression as a response of the equalization of the pressure in the inclusions and the outer pressure on the host mineral (Roedder, 1984). Decrepitation processes and their influence on the composition of fluid inclusions in quartz are examined quite thoroughly (see, for example, Roedder, 1984; Audetat and Gunther, 1999; Vityk *et al.*, 2000). We are not aware of any publications devoted to the decrepitation of melt inclusions, except only for papers merely mentioning of this process (see, for example, Roedder, 1984). In the context of our paper, which is not intended to exhaustively describe this problem, we attempted to principally characterize the effect of decrepitation on the composition of homogenized inclusions.

The system of inclusions can be opened through the diffusion of components from them, by the origin or reactivation of dislocations in the host mineral around these inclusions, or by brittle deformations of the host mineral, all of which are different stages of the same process (Vityk *et al.*, 2000). An obvious indication of decrepitation, which was established for inclusions in avachites, is the development of aureoles of secondary inclusions that contain melt in addition to a gas phase. Because decrepitation resulted in a pressure decrease in the melt inclusion, it lost volatile components whose solubility strongly depends on pressure (H_2O and CO_2). The very low H_2O contents (<0.1 wt %) measured in the melt inclusions seem not to correspond to the original concentrations of this component in the melts. Evaluations based on the IR spectroscopy of the olivine point to values of no less than 0.5 wt %, which can be regarded as the minimum estimate for the water contents in the parental melts of avachites. With a change in the external conditions, the olivine could also lose significant amounts of its original hydrogen content (Matveev *et al.*, 2005). Nevertheless, data obtained on avachites indicate that water can be preserved in olivine more efficiently than in melt inclusions. The IR spectroscopic examination of olivine provides new reliable information on the fluid regime of magma crystallization, with this information often lost from melt and fluid inclusions.

The decrepitation of inclusions is associated with an increase in their volume relative to that immediately after its isolation by the host mineral. Inclusions that underwent these transformations can be completely homogenized (with the dissolution of their gas bubbles) only at temperatures much higher than the temperatures of their capture by the olivine or cannot be homogenized at all because of the distortion of the required volume constancy of the inclusion after its capture by the host crystal (Roedder, 1984). None of the inclusions in olivine from avachites was completely homogenized, which provides additional evidence that the inclusions had been reopened and had lost part of their volatile components.

Some of the inclusions in olivine are significantly decrepitated, a process that was associated with brittle deformations in the olivine and the development of extensive halos of secondary melt and fluid inclusions (Fig. 1f). These inclusions were rejected from our experimental study. The secondary halos around the inclusions that were examined consisted of tiny inclusions, whose total mass was much smaller than the mass of the parental inclusion (Figs. 1a–1c). Nevertheless, we cannot completely rule out the removal of some melt amounts from the inclusions, and the effect of this process on the bulk composition of the inclusions should be evaluated.

The analysis of the possible decrepitation scenarios indicates that the influence of this process on the bulk composition of melt inclusions is variable and is controlled mostly by the occurrence and composition of daughter crystalline phases in the inclusions. If decrepitation occurred within the stability field of olivine as the only phase in equilibrium with the melt, this process should have led to the loss of volatile components, but the composition of the residual melt in the inclusion remained unchanged. The original composition of these inclusions can be reconstructed using techniques

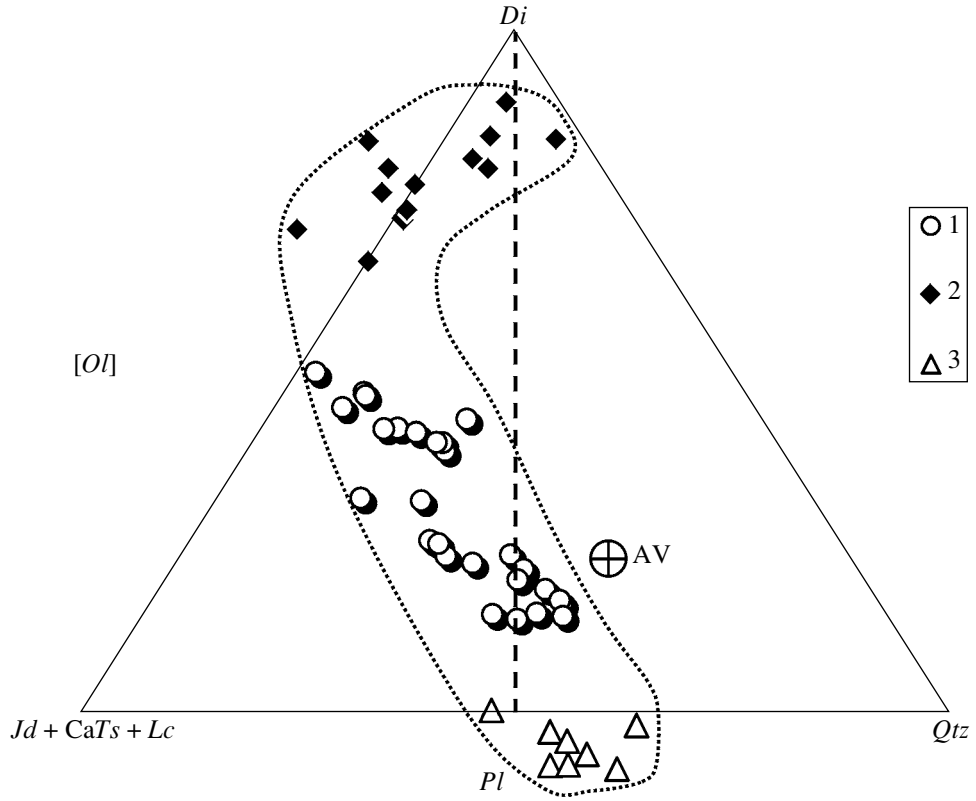

Fig. 12. Composition of partly homogenized melt inclusions and daughter phases in projection in the normative basaltic tetrahedron olivine [*Ol*]–quartz [*Qtz*]–diopside [*Di*]–jadeite + Ca-tschermakite + leucite [*Jd* + Ca*Ts* + *Lc*] from the *Ol* apex (Falloon and Green, 1987).

(1) Homogenized inclusions; (2) daughter clinopyroxene in inclusions; (3) residual glasses in inclusions, AV are the parental melts of avachites (AV-91 and AV-94) calculated from rock compositions (Portnyagin *et al.*, 2005). The projected normative compositions extend outside the tetrahedron because the normative compositions contained larnite (negative *Qtz* contents) and corundum (negative *Di* contents), which were not included in the calculations.

of mathematical simulation for the magmatic crystallization of olivine (see, for example, Danyushevsky *et al.*, 2003). The decrepitation of significantly recrystallized inclusions should have shifted their bulk composition toward higher contents of components contained in the daughter crystalline phases. The possibility of this process is clearly demonstrated in Fig. 1f, which exhibits an inclusion whose proportions of pyroxene and fluid are anomalously high relative to the amount of glass. It is impossible to reproduce the original composition of such inclusions by simulation techniques.

As was demonstrated in Section 5.1, the partly homogenized inclusions are characterized by a strong negative correlation between the contents of CaO and SiO_2 (Fig. 6), which is in principle consistent with the melting trend of the daughter pyroxene in inclusions. In this context, it is crucial to elucidate as to whether the decripitation process can account for the differences between the bulk compositions of the inclusions and rocks. In Fig. 12, the compositions of the daughter phases of the melt inclusions and the partly homogenized inclusions are shown in projection from the apex of the olivine-normative basalt tetrahedron (Falloon and Green, 1987). This projection is convenient in the context of the problem discussed here because it eliminates the effect of olivine melted from the inclusion walls during the experiment and the effect of reequilibration of the inclusion with olivine (see Section 7.2) on the measured composition of the inclusions. In this projection, the compositions of the homogenized inclusions plot between the compositions of the daughter pyroxene and residual glasses. Since these phases are, along with olivine, predominant in the recrystallized inclusions, this result confirms only the fact of the efficient homogenization of the inclusion during the experiment.

The most important inference from Fig. 12 is that practically all of the inclusions are undersaturated with SiO_2 and contain normative nepheline. The potential parental melt of avachites (AV-91, Table 1) is, conversely, hypersthene-normative and plots outside the field of the melt inclusions and their daughter phases. As can be seen from the simple geometric construction in Fig. 12, the crystallization or excess melting of daughter phases in the inclusions cannot lead to the der-

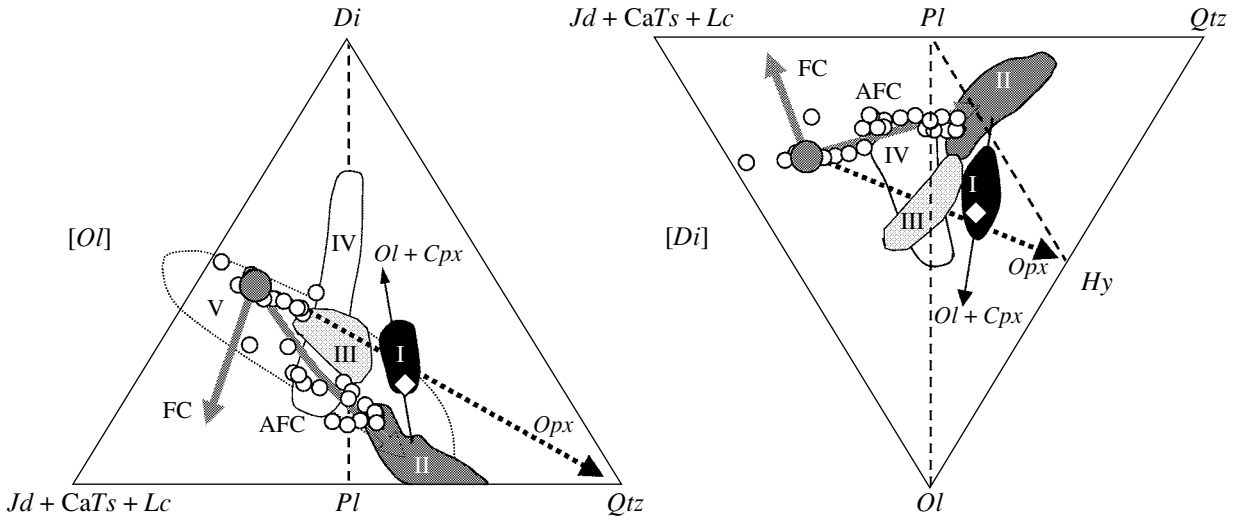

Fig. 13. Composition of melt inclusions in olivine from avachites recalculated to equilibrium with the host mineral and plotted in projection of the normative basaltic tetrahedron olivine [*Ol*]–quartz [*Qtz*]–diopside [*Di*]–jadeite + Ca-tschermakite + leucite [*Jd* + Ca*Ts* + *Lc*] from the *Ol* (left) and *Di* (right) apices (Falloon and Green, 1987).

Fields: I—avachites, II—lavas of Avachinsky volcano (Castellana, 1998), III—arc ankaramites (Green *et al.*, 2004), IV—compositions of melts produced by the partial melting of clinopyroxenite under pressures of 1–2 GPa (Kogiso and Hirschmann, 2001), V–partial melts derived from peridotite at $CO_2/H_2O > 0.4$ in the fluid phase (Mysen and Boettcher, 1975). Larger circles mark the average composition of inclusions in the most magnesian olivine (*Fo* > 90 mol %). Diamond shows the composition of the avachite parental melt AV-94 calculated from the compositions of the rocks (Portnyagin *et al.*, 2005). Arrows correspond to melt compositional trends during the cotectic crystallization of olivine and pyroxene (*FC*) and the hypothetical trend of crystallization coupled with the assimilation of the wall rocks (*AFC*). The arrow labeled (*Ol* + *Cpx*) indicates the shift of the rock compositions during olivine and pyroxene accumulation, which explains the bulk composition of avachites. The dotted arrow labeled (*Opx*) corresponds to orthopyroxene control of the composition of the avachite parental melt (see Section 7.5. in text).

ivation of silica-undersaturated melts from composition AV-91 or the compositions of the rocks. Thus, it follows that decrepitation cannot account for the unusual composition of the melt inclusions, which was originally different from the composition of the rocks.

At the same time, the possible influence of decrepitation on the composition of the silicate constituent of inclusions cannot be ruled out on the basis of the data of Fig. 12. The bulk composition of the inclusions containing (because of decrepitation) anomalously high amounts of daughter pyroxene should plot within the same field as the compositions of the primary inclusions but has to be shifted toward the *Di* apex. The local variations in the CaO concentrations of inclusions in the same olivine grain (for instance, inclusions in grain 4, Table 3) can likely be explained by decrepitation processes, but the general systematics of the compositions of the inclusions in different olivine grains should have been controlled by other processes.

7.5. Parental Melts of Avachites

The composition of melt inclusions from avachites underwent certain transformations after the capture of these inclusions due to their reequilibration with the host olivine, crystallization, and decrepitation. The influence of these processes on the composition of the inclusions was taken into account, and the results thus obtained indicate that the olivine of avachites crystallized from compositionally diverse melts, most of which have no analogues among the rocks of Avachinsky volcano (Figs. 5, 13).

The composition of the parental melt of avachites obtained by averaging the compositions of melt inclusions in the most magnesian olivine (*Fo* > 90 mol %) is shown in Table 1 (composition AV-I). Compared with the estimates based on the rock compositions (AV-91 and AV-94; Portnyagin *et al.*, 2005), the primitive melt inclusions are richer in CaO, Al_2O_3, and Na_2O at low SiO_2 and MgO concentrations and have a nepheline-normative composition. As was mentioned in Section 7.4, these differences cannot be explained by the crystallization of olivine and/or clinopyroxene and testify that the evolutionary path of the avachite magmas was more complicated than can be inferred from the compositions of the rocks and their minerals (Portnyagin *et al.*, 2005).

An interesting inference from the analysis of the differences between the normative compositions of the parental magmas of avachites in projections within the basalt tetrahedron (Fig. 13) is as follows: the difference between these compositions was caused by the strong depletion of melt AV-I in components contained in orthopyroxene. In other words, the hypothetically possible processes of orthopyroxene dissolution in melt AV-I could result in melt AV-94, or, conversely, ortho-

pyroxene crystallization from melt AV-94 can explain the origin of melt AV-I. However, orthopyroxene as a modal phase was not found among either the phenocrysts of avachites or the solid inclusions in olivine (Portnyagin *et al.*, 2005). The genetic role of orthopyroxene control over the composition of the avachite parental melts is a task for forthcoming studies.

Independent evidence of the crystallization of olivine in avachites from low siliceous magmas is the position of the absorption bands of the OH^- group in the IR spectra of this mineral. Such spectra are typical of olivine crystallizing from a melt at a low silica activity and differ from the position of these spectral bands for olivine that was in equilibrium with orthopyroxene (Matveev *et al.*, 2001). Magnesian basalts from Avachinsky volcano could be generated with the participation of magmas of ankaramite composition (Portnyagin *et al.*, 2005). Conceivably, inclusions in olivine from avachites can be portions of these primitive ankaramite melts. Nevertheless, none of the rocks of Avachinsky volcano correspond in composition to the high-Ca melt inclusions. This fact puts forth two principal and interrelated problems: (i) of the genesis of the ankaramite magmas and their role in the processes of island-arc petrogenesis and (ii) of the genetic links between silica-undersaturated ankaramite magmas and basalts and andesites of typical quartz- and hypersthene-normative composition.

The high-Ca compositions discovered in the course of our investigation are not the first find of such compositions as inclusions in arc lavas. Similar melts were described in Indonesia (Sisson and Bronto, 1998), Vanuatu (Della-Pasqua and Varne, 1997), Philippines (Schiano *et al.*, 2000), Central America (Walker *et al.*, 2003), and Italy (Gioncada *et al.*, 1998) and also occur as an extensive population of inclusions in olivine from Klyuchevskoi volcano (Mironov *et al.*, 2003). In all of these instances, the olivine hosting high-Ca inclusions is highly magnesian ($Fo_{85–94}$). Inclusions in more ferrous olivine usually have compositions close to those of the corresponding rocks (Schiano *et al.*, 2000; Mironov *et al.*, 2001). Inclusions in olivine from avachites are not exception to this rule (Fig. 5).

It was hypothesized (Schiano *et al.*, 2000) that nepheline-normative arc melts are produced by the partial melting of cumulative clinopyroxenites in the lower crust or upper mantle. Later experiments have not confirmed the possibility of the origin of strongly silica-undersaturated melt as a result of this process (Kogiso and Hirschmann, 2001) (Fig. 13). These experiments were conducted under dry conditions, and it cannot be ruled out that an increase in the contents of volatiles (H_2O and CO_2) can lead to closer similarities between their results and the natural data, although this should be confirmed experimentally. It is also pertinent to mention that, during 20–40% partial melting of clinopyroxenite, liquidus olivine in most of the experiments (Kogiso and Hirschmann, 2001) was more ferrous ($Fo_{77–87}$) than olivine in avachites and other primitive arc rocks. Highly magnesian olivine ($Fo_{88–91}$) was obtained only at degrees of melting greater than 60% and temperatures of more that 1400°C. The compositions of these high-temperature melts approach that of the source pyroxenite and principally differ from the highly calcic melt inclusions in having lower contents of alumina and alkalis.

It was hypothesized (Danyushevsky *et al.*, 2003, 2004) that olivine can preferably trap inclusions of foreign (including highly calcic) composition because of the rapid growth in the marginal parts of magmatic bodies, where assimilation of the host rocks was highly probable. Because of their selective capture, the inclusions may be not adequately enough representative for the characterization of the composition of large magma volumes. Critically analyzing this ingenious idea, it should be mentioned that the assimilation of host rocks is an energy-consuming process (see, for example, Bohrson and Spera, 2001), and, thus, assimilation processes should expectedly be associated with a rapid growth of minerals not only at the assimilation front but also away from it. Inclusions captured in minerals should have variable compositions, including those not affected by assimilation. In fact, there are exclusively Ca-rich compositions in the high-Mg olivines of avachites, but no evidence has been found that primitive melts of other composition, close to those of the rocks exist.

Note that crustal assimilation should, perhaps, have modified the composition of the primitive magmas regardless of the processes of mantle magma generation and the characteristics of the parental melts. Our data on the composition of melt inclusions from lavas of Nachikinskii volcano, the northernmost Quaternary volcano in Kamchatka, which developed on the crust of thickness and composition typical of Kamchatka, indicate that the primitive melts of this volcano had a nepheline- and hypersthene-normative low-Ca (CaO/Al_2O_3 = 0.53–0.72) composition and were produced by the decompressional melting of the mantle in the absence of subducted material (Portnyagin *et al.*, 2003). The finds of melt inclusions of ankaramite composition are of systematic character only at volcanoes whose magmas were generated in environments of active subduction, such as Avachinsky and Klyuchevskoi volcanoes in Kamchatka. Proceeding from these observations, we suggest that the occurrence of high-Ca melts most probably reflects the magma generation conditions in the mantle wedges above subduction zones and is not related to crustal assimilation.

The idea that nepheline-normative ankaramite melts can be generated by the partial melting of mantle wedges above subduction zones was put forth in (Della-Pasqua and Varne, 1997). These researchers proposed that high and moderate CO_2 concentrations and CO_2/H_2O ratios in the fluid are able to shift the composition of the partial melts toward higher contents of clinopyroxene than those in the melting products of both

dry and H_2O-rich peridotites (Brey and Green, 1975; Mysen and Boetcher, 1975). The melts obtained experimentally under pressures of 2.5–3.5 GPa, in the garnet stability field, have a low-Al melilitite composition (CaO/Al_2O_3 = 0.9–2.2) Brey and Green, 1975; Hirose, 1997) and notably differ from the primitive ankaramite melts of island arcs (Schiano *et al.*, 2000) and from avachite melts obtained in this research. Experiments (Mysen and Boetcher, 1975) under pressures of 0.75–2.2 GPa demonstrate an obvious shift of the mantle melts to the field of nepheline-normative ankaramite magmas at an increase in the CO_2/H_2O ratio in the fluid. The glasses generated at 1.0 and 2.0 GPa and CO_2/H_2O = 0.5 show close compositional similarities with parental melt AV-I. However, the poor quenching of the experimental glasses in (Mysen and Boetcher, 1975) does not permit any reliable comparison. Experimental data (Green *et al.*, 2004; Schmidt *et al.*, 2004) newly obtained on the melting of depleted lherzolite at variable CO_2/H_2O ratios and pressures of 1.5–2.0 GPa demonstrate that the melts have Ca-rich compositions but all are hypersthene-normative. One of the conclusions in (Schmidt *et al.*, 2004) is that nepheline-normative ankaramites can hardly be derived from a magma source containing orthopyroxene. Obviously, this conclusion is in conflict with the earlier experimental results in (Mysen and Boetcher, 1975).

Thus, the scarcity of experimental data on the melting of compositionally diverse upper mantle rocks (clinopyroxenite, wehrlite, and peridotite) at variable CO_2/H_2O ratios in the fluid still does not allow a reliable evaluation of the possible conditions of the origin of primitive avachite melts. It is most probable that these melts were derived by the melting of a high-Mg peridotite source, with the residue containing olivine $Fo_{90–91}$, under a high CO_2 partial pressure. This process resulted in an increase in clinopyroxene content at the expense of orthopyroxene in the equilibrium peridotite melt.

A possible source of primitive avachite melts could be mantle peridotite extensively metasomatized by a carbonatite component (Green *et al.*, 2004). The rocks of subducted oceanic plates are rich in carbonate material (Alt and Teagle, 1999). The decarbonatization of subducted-plate material can give rise to carbonatite melts, which can then migrate to higher stratigraphic levels of the mantle wedge (Kerrick and Connolly, 2001). Reactions between the silica-undersaturated carbonatite melts and peridotite should have resulted in the metasomatic enrichment of the peridotite and, perhaps, the origin of olivine, clinopyroxene, and/or amphibole instead of orthopyroxene. At a significant progress of this reaction, the peridotite can be modified into wehrlite. The subsequent involvement of the heterogeneously metasomatized peridotite in partial melting can account for the development of geochemically diverse melts, including nepheline-normative ankaramite magmas.

Along with the apparent differences of the avachite primitive melts from the rocks in terms of major components, it should be mentioned that these melts are also characterized by significant variations in the contents of trace elements incompatible with olivine or pyroxene (Figs. 6, 9). The origin of melts variably enriched in incompatible trace elements can also be explained by the appearance of heterogeneously metasomatized peridotite, in addition to possible variations in the degrees of peridotite partial melting. The geochemical variability of the parental magmas of avachites in terms of incompatible elements will be discussed in detail in our future papers.

7.6. Parental Melt Evolution and Avachite Genesis

The main liquidus phases of the avachite parental melts were olivine and clinopyroxene. If these melts were strongly undersaturated with SiO_2 (see above), olivine and clinopyroxene crystallization alone could not bring the derivatives into the region of hypersthene- and quartz-normative compositions and account for the origin of the typical lavas of Avachinsky volcano (Fig. 13). The crystallization of significant amounts of spinel and magnetite, together with silicate minerals can induce an increase in the SiO_2 content in the melt. In this case, it is reasonable to expect that the FeO* and TiO_2 contents of the weakly differentiated melts decreased, which is at variance with the actual situation (Fig. 5). Magnetite is one of the main liquidus phases of the Avachinsky andesites but is atypical of the basalts (see Fig. 2 in Portnyagin *et al.*, 2005). An alternative explanation can be the significant assimilation of crustal material by the magmas, a process that can explain both the general tendency in magma fractionation into the region of quartz-normative compositions (Fig. 13) and the significant unsystematic variations in the SiO_2 contents in the melt inclusions captured in olivine grains with similar Mg# (Fig. 5). If the hypothesis of crustal contamination during the fractionation of the avachite parental magmas is valid, this process should be spread much more widely during the fractionation of basaltic magmas in island arcs than was thought previously. The validation of this hypothesis calls, however, for more detailed studying the concentrations of trace elements and isotopic ratios of the melts and minerals.

The evaluated crystallization temperatures and pressures of the melts are listed in Table 6. Portnyagin *et al.* (2005) suggested that the crystallization trajectories of the avachite parental melts are decompressional. The data obtained using the compositions of melt inclusions only partly confirm this hypothesis. The magmas crystallized under different pressures (0–1.2 GPa), but there is no correlation between the pressure estimates for the equilibria of melt with olivine and clinopyroxene and the composition of the olivine that hosts the melts (Fig. 14). Although the number of the analyzed inclusions is not great, our data testify that the more probable genesis of the rocks was the fractionation of different

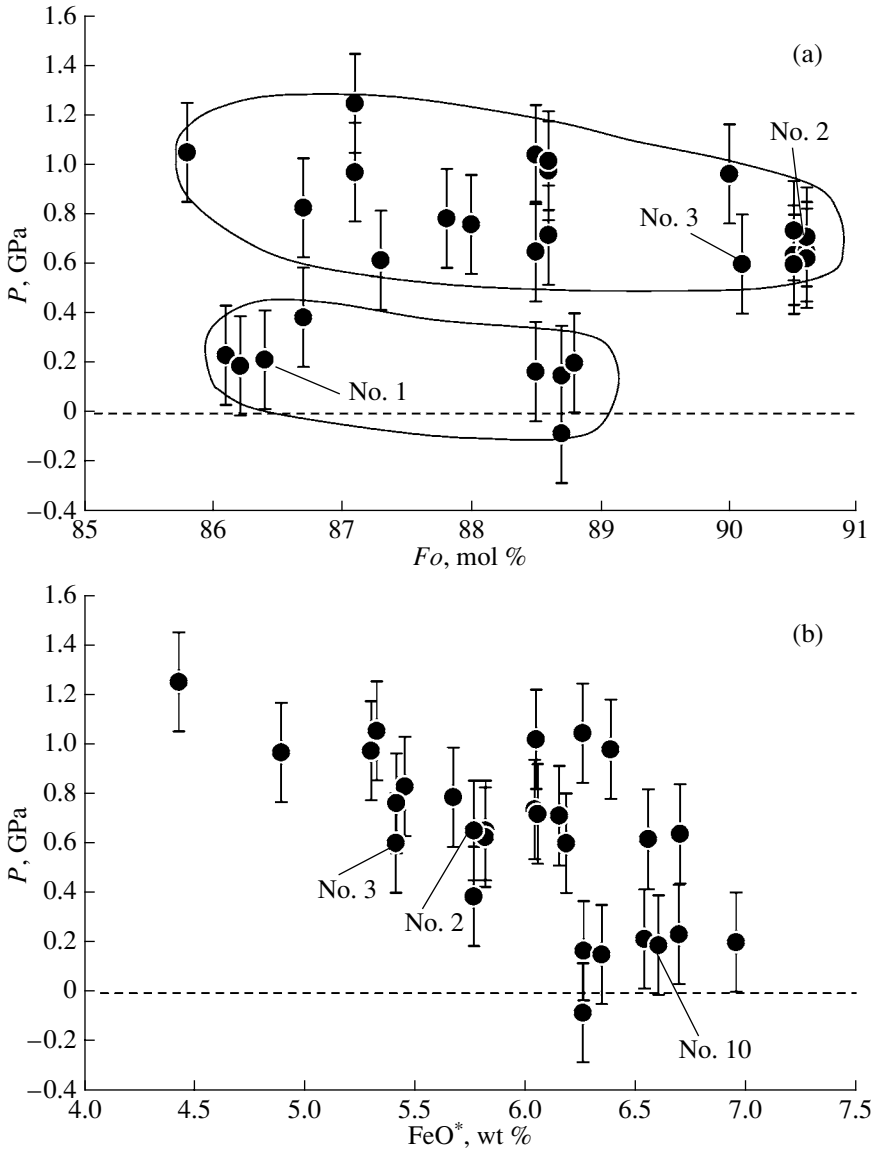

Fig. 14. Dependence of the pressure of equilibrium between melt in the inclusions with the olivine–pyroxene phenocryst assemblage and the composition of (a) the host olivine and (b) the measured FeO* content in the melt.
Numerals correspond to the numbers of inclusions whose evolutionary history was reconstructed in detail.

portions of the parental magmas at different depth levels. The melts can be provisionally subdivided into two groups, which crystallized at pressures of >0.5 GPa and <0.5 GPa, near the surface. It is worth mentioning that there is a significant correlation between the pressures evaluated for equilibria of the parental melts and the FeO* contents measured in the homogenized inclusions. The latter parameter is indicative, as was mentioned above, of the degree of reequilibration between the inclusions and olivine and is a function of the absolute time during which the phenocrysts resided in the cooling magma (Fig. 14). The time during which the olivines crystallizing at greater depths occurred in the magma was at least one order of magnitude longer (see, for example, grains 2 and 3, Section 7.2) than the residence time of the olivines that crystallized in another magma near the surface immediately before the eruption (see, for example, grain 10, Section 7.2).

The observations described above can be explained within the scope of a general model for the genesis of avachites (Fig. 15). It is thought that the magma portion (or portions) initially intruded into the lower crust beneath Avachinsky volcano had a Ca-rich composition and crystallized at depths of 20–30 km. Its crystallization was associated with crustal assimilation and the origin of olivine–pyroxene cumulates. During the second stage, the arrival of new magma portions temporarily stopped. The earlier cumulates cooled and compacted, and their interstitial melt crystallized. The cooling of the cumulates was accompanied by the

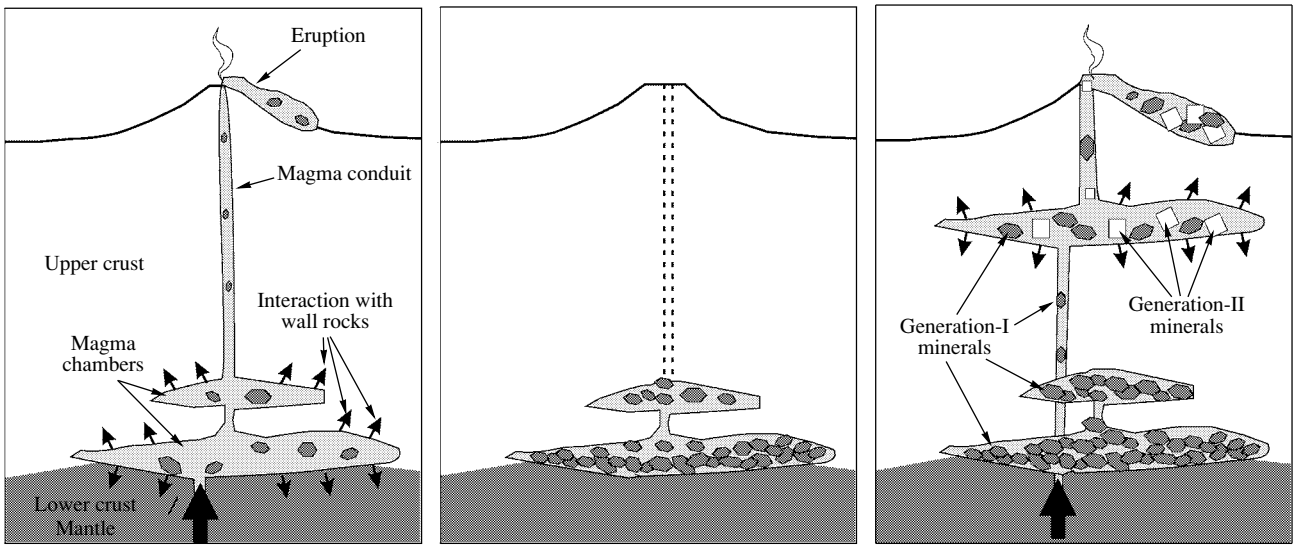

Fig. 15. Schematic model proposed for the origin of avachites as a result of the multistage differentiation of the parental magmas in the crust.

reequilibration of melt inclusions in the olivine. During the third stage, new magma portions were intruded and interacted *en route* to the surface with the earlier cumulates. This magma entrained olivine and pyroxene crystals and brought them to the upper levels of the feeding system of the volcano. This stage was likely marked by brittle deformations and the fracturing of crystals, the origin of crystals with complex and reverse zoning, and the entrapment of host-rock xenoliths that are contained in avachites (Portnyagin *et al.*, 2005). The crystallization of the magma and the concurrent assimilation of the host rocks took place in a shallower chamber or a magma conduit *en route* to the surface. The eruption of the hybrid magmas with fragments of the older cumulates and minerals that crystallized from the transporting magma itself gave rise to avachites.

8. CONCLUSIONS

The detailed study of melt inclusions in the olivine phenocrysts led us to the following conclusions about the genesis of avachites, unique high-Mg rocks in eastern Kamchatka.

(1) In contrast to the rocks, the parental melts of avachites were strongly undersaturated with SiO_2 and had a high-Ca composition close to that of nepheline-normative ankaramites. It is thought that the parental ankaramitic magmas were derived by the partial melting of a peridotite source that had been metasomatized by a carbonatite component. The genesis of the latter was related to the subduction of the oceanic lithosphere beneath Kamchatka.

(2) The melts crystallized in magma chambers at different depths and simultaneously assimilated the host crustal rocks. The phenocryst minerals of avachites were determined to have crystallized in two stages, during which the early olivine–pyroxene cumulates were produced and subsequently remobilized and transported to the surface together with a newly arriving magma portion. Avachites are hybrid cumulative rocks produced in a long-lived open magmatic system.

(3) Numerous finds of ankaramite melts in inclusions in magnesian olivine from Kamchatka and other active continental margins suggest that ankaramite magmas can be a widespread type of parental arc magmas. Genetic links between ankaramites and the rocks of typical differentiated silica-saturated composition can be explained by the significant assimilation of the host rocks during the differentiation of the parental mantle melts.

The petrological conclusions of this research are based on the thorough analysis of the processes that could modify the original composition of the inclusions after their capture by the host minerals. The crystallization trajectories of the inclusions and the melts around their host crystals are demonstrated to have been different. The possible reasons for these differences are ana-

lyzed, and the possible consequences of the decrepitation of melt inclusions in the olivine are characterized. A method is described that can be used to reproduce the cooling history of olivine phenocrysts with melt inclusions, along with the possible application of the information thus obtained to the solution of petrological problems. The results of our research contribute to the development of methods used in the studying of melt inclusions, a unique technique for the reconstruction of petrological information that was obliterated from the bulk compositions of magmatic rocks.

ACKNOWLEDGMENTS

The authors thank A.B. Osipenko (Vernadsky State Geological Museum, Russian Academy of Sciences) for providing avachite samples, N.N. Kononkova (Vernadsky Institute of Geochemistry and Analytical Chemistry, Russian Academy of Sciences), N.N. Korotaeva (Moscow State University), A. Krontz (Geochemical Institute, Göttingen), and M. Töner (IfM-GEOMAR) for help with microprobe analyses. S.G. Simakin and E. Potapov (Institute of Microelectronics, Russian Academy of Sciences) are thanked for conducting ion-microprobe analyses. We appreciate the possibility of working at the Geochemical Institute in Göttingen provided for us by courtesy of G. Werner (Geochemical Institute, Göttingen). L.V. Danyushevsky (Tasmania University, Australia) is thanked for offering the possibility of using the computer programs Petrolog 2.0 and Fe-LOSS and for help in familiarizing with them. We thank V.B. Naumov (Vernadsky Institute of Geochemistry and Analytical Chemistry, Russian Academy of Sciences) for help in conducting cryometric experiments and fruitful discussion and A.V. Girnis (Institute of the Geology of Ore Deposits, Petrography, Mineralogy, and Geochemistry, Russian Academy of Sciences) for constructive comments on an earlier version of the manuscript. This study was supported by the Russian Foundation for Basic Research, project no. 03-05-64629 and the Ministry of Science and Education of Germany (BMBF), grant KOMEX-2. Additional support from the Russian Scientific School Program (grants 1831.2003.5 and 1645.2003.5b) is kindly acknowledged.

REFERENCES

1. J. C. Alt and D. H. Teagle, "The Uptake of Carbon during Alteration of Ocean Crust," Geochim. Cosmochim. Acta **63** (10), 1527–1535 (1999).
2. V. V. Anan'ev and G. D. Shnyrev, "Garnet in Melt Inclusions from Olivine of *Ol–An* Aggregates, Ksudach Volcano, Kamchatka," Dokl. Akad. Nauk SSSR **274** (2), 402–406 (1984).
3. A. Audetat and D. Gunther, "Mobility and H_2O Loss from Fluid Inclusions in Natural Quartz Crystals," Contrib. Mineral. Petrol. **137**, 1–14 (1999).
4. W. A. Bohrson and F. J. Spera, "Energy-Constrained Open-System Magmatic Processes II: Application of Energy-Constrained Assimilation–Fractional Crystallization (EC-AFC) Model to Magmatic Systems," J. Petrol. **42**, 1019–1040 (2001).
5. G. Brey and D. H. Green, "The Role of CO_2 in the Genesis of Olivine Melilite," Contrib. Mineral. Petrol. **49**, 93–103 (1975).
6. B. Castellana, PhD Thesis (Univ. California, Los Angeles, 1998).
7. L. V. Danyushevsky, R. A. Leslie, A. J. Crawford, and P. Durance, "Melt Inclusions in Primitive Olivine Phenocrysts: the Role of Localized Reaction Process in the Origin of Anomalous Compositions," J. Petrol. **45**, 2531–2553 (2005).
8. L. V. Danyushevsky, F. N. Della-Pasqua, and S. Sokolov, "Re-Equilibration of Melt Inclusions Trapped by Magnesian Olivine Phenocrysts from Subduction-related Magmas: Petrological Implications," Contrib. Mineral. Petrol. **138**, 68–83 (2000).
9. L. V. Danyushevsky, A. W. McNeill, and A. V. Sobolev, "Experimental and Petrological Studies of Melt Inclusions in Phenocrysts from Mantle-Derived Magmas: An Overview of Techniques, Advantages, and Complications," Chem. Geol. **183**, 5–24 (2002a).
10. L. V. Danyushevsky, A. V. Sobolev, and L. V. Dmitriev, "Estimation of the Pressure of Crystallization and H_2O Content of MORB and BABB Glasses: Calibration of an Empirical Technique," Mineral. Petrol. **57**, 185–204 (1996).
11. L. V. Danyushevsky, S. Sokolov, and T. Falloon, "Melt Inclusions in Phenocrysts: Using Diffusive Re-Equilibration to Determine the Cooling History of a Crystal, with Implications for the Origin of Olivine-Phyric Volcanic Rocks," J. Petrol. **43**, 1651–1671 (2002b).
12. L. V. Danyushevsky, M. R. Perfit, S. M. Eggins, and T. J. Falloon, "Crustal Origin for Coupled 'Ultra-Depleted' and 'Plagioclase' Signatures in MORB Olivine-Hosted Melt Inclusions: Evidence from the Siqueiros Transform Fault, East Pacific Rise," Contrib. Mineral. Petrol. **144**, 619–637 (2003).
13. F. N. Della-Pasqua and R. Varne, "Primitive Ankaramitic Magmas in Volcanic Arcs: A Melt-Inclusion Approach," Can. Mineral. **35**, 291–312 (1997).
14. F. N. Della-Pasqua, V. S. Kamenetsky, M. Gasparon, *et al.*, "Al-Spinels in Primitive Arc Volcanics," Mineral. Petrol. **53**, 1–26 (1995).
15. EarthRef (Earth Reference Data and Models), Website http://www.earthref.org/ 2004 (accessed).
16. T. J. Falloon and D. H. Green, "Anhydrous Partial Melting of MORB Pyrolite and Other Peridotite Compositions at 10 Kbar: Implication for the Origin of Primitive MORB Glasses," Mineral. Petrol. **37**, 181–219 (1987).
17. T. J. Falloon and L. V. Danyushevsky, "Melting of Refractory Mantle at 1.5, 2, and 2.5 GPa under Anhydrous and H_2O-undersaturated Conditions: Implications for the Petrogenesis of High-Ca Boninites and the Influence of Subduction Components on Mantle Melting," J. Petrol. **412**, 257–283 (2000).
18. C. E. Ford, D. G. Russel, J. A. Graven, and M. R. Fisk, "Olivine–Liquid Equilibria: Temperature, Pressure, and Composition Dependence of the Crystal/Liquid Cation Partition Coefficients for Mg, Fe^{2+}, Ca, and Mn," J. Petrol. **24**, 256–265 (1983).

19. M.-L. Frezzotti, "Silicate-Melt Inclusions in Magmatic Rocks: Applications to Petrology," Lithos **55**, 273–299 (2001).

20. G. A. Gaetani and E. B. Watson, "Open System Behavior of Olivine-Hosted Melt Inclusions," Earth Planet. Sci. Lett. **183**, 27–41 (2000).

21. J. B. Gill, *Orogenic Andesites and Plate Tectonics* (Springer-Verlag, Berlin, 1981).

22. A. Gioncada, R. Clocchiatti, A. Sbrana, *et al.*, "A Study of Melt Inclusions at Volcano (Aeolian Islands, Italy): Insights on the Primitive Magmas and on the Volcanic Feeding System," Bull. Volcanol. **60**, 286–306 (1998).

23. D. H. Green, M. W. Schmidt, and W. O. Hibberson, "Island-Arc Ankaramites: Primitive Melts from Fluxed Refractory Lherzolitic Mantle," J. Petrol. **45**, 391–403 (2004).

24. A. A. Gurenko, A. V. Sobolev, A. I. Polyakov, and N. N. Kononkova, "Parental Melt of Rifting-Related Tholeiites in Iceland: Composition and Crystallization Conditions," Dokl. Akad. Nauk SSSR **301** (1), 179–184 (1988).

25. K. Hirose, "Partial Melt Compositions of Carbonated Peridotite at 3 GPa and Role of CO_2 in Alkali-basalt Magma Generation," Geophys. Res. Lett. **24** (Iss. 22), 2837–2840 (1997).

26. A. W. Hofmann, "Chemical Differentiation of the Earth: The Relationship between Mantle, Continental Crust, and Oceanic Crust," Earth Planet. Sci. Lett. **90**, 297–314 (1988).

27. A. W. Hofmann, "Mantle Geochemistry: The Message from Oceanic Volcanism," Nature **385**, 219–229 (1997).

28. E. J. Jarosewich, J. A. Nelen, and J. A. Norberg, "Reference Samples for Electron Microprobe Analysis," Geostand. Newslett. **4**, 43–47 (1980).

29. D. M. Kerrick and J. A. D. Connolly, "Metamorphic Devolatilization of Subducted Oceanic Metabasalts: Implications for Seismicity, Arc Magmatism, and Volatile Recycling," Earth Planet. Sci. Lett. **189**, 19–29 (2001).

30. T. Kogiso and M. M. Hirschmann, "Experimental Study of Clinopyroxenite Partial Melting and the Origin of Ultra-calcic Melt Inclusions," Contrib. Mineral. Petrol. **142**, 347–360 (2001).

31. F. Sh. Kutyev, B. V. Ivanov, A. A. Ovsyannikov, *et al.*, "Exotic Lavas of the Avachinskii Volcano," Dokl. Akad. Nauk SSSR **255** (5), 1240–1243 (1980).

32. D. Kuzmin and A. Sobolev, "Boundary Layer Effect on the Composition of Melt Inclusions in Olivine," Geophys. Res. Abstr. **5** (05665) (2003).

33. G. Libourel, "Systematics of Calcium Partitioning between Olivine and Silicate Melt: Implications for Melt Structure and Calcium Content of Magmatic Olivines," Contrib. Mineral. Petrol. **136**, 63–80 (1999).

34. S. Matveev, H. S. C. O' Neill, C. Ballhaus, *et al.*, "Effect of Silica Activity on OH-IR Spectra of Olivine: Implications for Low-$a$$SiO_2$ Mantle Metasomatism," J. Petrol. **42**, 721–729 (2001).

35. S. Matveev, M. V. Portnyagin, C. Ballhaus, *et al.*, "FTIR Spectrum of Phenocryst Olivine as an Indicator of Silica Saturation in Magmas," J. Petrol. **46**, 603–614 (2005).

36. N. Metrich and R. Clocchiatti, "Sulfur Abundance and Its Speciation in Oxidized Alkaline Melts," Geochim. Cosmochim. Acta **60**, 4151–4160 (1996).

37. N. Mironov, M. Portnyagin, and P. Pletchov, "The Origin and Composition of Primitive Melts of Klyuchevskoy Volcano, Kamchatka: Insight from Melt Inclusions Study," Geophys. Res. Abstr. **5** (01966) (2003).

38. N. L. Mironov, M. V. Portnyagin, P. Yu. Plechov, and S. A. Khubunaya, "Final Stages of Magma Evolution in Klyuchevskoy Volcano, Kamchatka: Evidence from Melt Inclusions in Minerals of High-alumina Basalts," Petrologiya **9** (1), 51–69 (2001) [Petrology **9** (1), 46–62 (2001)].

39. M. Mosbah, N. Metrich, and P. Massiot, "PIGME Fluorine Determination Using a Nuclear Microprobe with Application to Glass Inclusions," Nucl. Instrum. Methods Phys. Res. **58**, 227–231 (1991).

40. B. O. Mysen and A. L. Boettcher, "Melting of a Hydrous Mantle: I. Phase Relations of Natural Peridotite at High Pressures and Temperatures with Controlled Activities of Water, Carbon Dioxide, and Hydrogen," J. Petrol. **16**, 520–548 (1975).

41. M. J. O' Hara and C. Herzberg, "Interpretation of Trace Element and Isotope Features of Basalts: Relevance of Field Relations, Petrology, Major Element Data, Phase Equilibria, and Magma Chamber Modeling in Basalt Petrogenesis," Geochim. Cosmochim. Acta **66**, 2167−2191 (2002).

42. M. Portnyagin and K. Hoernle, "Reconstruction of the Cooling History and Initial FeO of Melt Inclusions from Alkaline Basalts of Nachikinsky Volcano (North Kamchatka)," Geophys. Res. Abstr. **5** (05821) (2003).

43. M. V. Portnyagin, K. Hoernle, and G. P. Avdeiko, "Evidence for Decompressional Melting of Garnet Peridotite at the Kamchatka–Aleutian Junction," Geochim. Cosmochim. Acta **67** (Suppl. 1), A381 (2003).

44. M. V. Portnyagin, P. Yu. Plechov, S. V. Matveev, *et al.*, Petrology of Avachites, High-Mg Basalts of Avachinsky Volcano, Kamchatka: I. General Characteristics and Compositions of Rocks and Minerals," Petrologiya **13**, 115–138 (2005) [Petrology **13**, 99–121 (2005)].

45. K. Putirka, M. Johnson, R. Kinzler, *et al.*, "Thermobarometry of Mafic Igneous Rocks Based on Clinopyroxene–Liquid Equilibria, 0–30 Kbar," Contrib. Mineral. Petrol. **123**, 92–108 (1996).

46. Z. Qin, F. Lu, and A. T. Anderson, Jr., "Diffusive Re-Equilibration of Melt and Fluid Inclusions," Am. Mineral. **77**, 565–576 (1992).

47. E. Roedder, *Fluid Inclusions*, Vol. 12 of *Reviews in Mineralogy* (Mineral. Soc. Am., Washington, 1984).

48. P. Schiano, J. M. Eiler, I. D. Hutcheon, and E. M. Stolper, "Primitive CaO-Rich, Silica-Undersaturated Melts in Island Arcs: Evidence for the Involvement of Clinopyroxene-Rich Lithologies in the Petrogenesis of Arc Magmas," Geochem. Geophys. Geosyst. **1** (1999GC000032) (2000).

49. M. W. Schmidt, D. H. Green, and W. O. Hibberson, "Ultra-calcic Magmas Generated from Ca-Depleted Mantle: An Experimental Study on the Origin of Ankaramites," J. Petrol. **45** (3), 531–554 (2004).

50. T. W. Sisson and S. Bronto, "Evidence for Pressure-Release Melting beneath Magmatic Arcs from Basalt at Galunggung, Indonesia," Nature **391**, 883–886 (1998).
51. A. V. Sobolev, "Melt Inclusions in Minerals as a Source of Principle Petrological Information," Petrologiya **4** (3), 228–239 (1996) [Petrology **4** (3), 209–220 (1996)].
52. A. V. Sobolev, L. V. Dmitriev, V. L. Barsukov, *et al.*, "The Formation Conditions of High Magnesium Olivines from the Monomineral Fraction of Luna-24 Regolith," in *Proceedings of the 11th Lunar Planetary Science Conference* (1980), pp. 105–116.
53. A. V. Sobolev, N. V. Sobolev, C. B. Smith, and J. Dubessy, "Fluid and Melt Compositions in Lamproites and Kimberlites Based on the Study of Inclusions in Olivine," in *Proceedings of the 4th International Kimberlite Conference*, Vol. 1 *Kimberlites and Related Rocks: Their Composition, Occurrence, Origin, and Emplacement*, Ed. by J. Ross (Blackwell, Boston, 1989), pp. 220–240.
54. S. Tait, "Selective Preservation of Melt Inclusion in Igneous Phenocrysts," Am. Mineral. **77**, 146–155 (1992).
55. Y. Tatsumi, M. Sakuyama, H. Fukuyama, and I. Kushiro, "Generation of Arc Basalt Magmas and Thermal Structure of the Mantle Wedge in Subduction Zones," J. Geophys. Res. **88**, 5815–5825 (1983).
56. M. L. Tolstykh, A. D. Babanskii, V. B. Naumov, *et al.*, "Chemical Composition, Trace Elements, and Volatile Components of Melt Inclusions in Minerals from Andesites of the Avachinskii Volcano, Kamchatka," Geokhimiya, No. 11, 1229–1237 (2002) [Geochem. Int. **40** (11), 1112–1120 (2002)].
57. M. O. Vityk, R. J. Badnar, and J.-C. Doukhan, "Synthetic Fluid Inclusions: XV. TEM Investigation of Plastic Flow Associated with Re-equilibration of Fluid Inclusions in Natural Quartz," Contrib. Mineral. Petrol. **139**, 285–297 (2000).
58. J. A. Walker, K. Roggensack, L. C. Patino, *et al.*, "The Water and Trace Element Contents of Melt Inclusions across an Active Subduction Zone," Contrib. Mineral. Petrol. **146**, 62–77 (2003).
59. P. Wallace and I. S. E. Carmichael, "Sulfur in Basaltic Magmas," Geochim. Cosmochim. Acta **56**, 1863–1874 (1992).